Aus der Kinderklinik und Kinderpoliklinik
im Dr. von Haunerschen Kinderspital
Klinik der Universität München
Direktor: Prof. Dr. Dr. Christoph Klein

Identification of TRIB1 as a Novel Regulator of the Secretory Pathway

Dissertation
zum Erwerb des Doktorgrades der Medizin
an der Medizinischen Fakultät der
Ludwig-Maximilians-Universität zu München

vorgelegt von

Anna Lu Gan

aus München

2023

Mit Genehmigung der Medizinischen Fakultät

der Universität München

Berichterstatter: Prof. Dr. Christoph Klein

Mitberichterstatter: PD Dr. Johanna Tischer

PD Dr. Dorit Nägler

Dekan: Prof. Dr. med. Thomas Gudermann

Tag der mündlichen Prüfung: 22.06.2023

Table of Contents

I List of Abbreviation 7

II Introduction 9

1 The Secretory Pathway 9
1.1 ER stress and homeostasis 10
1.2 The Golgi apparatus 11

2 The CRISPR/Cas9 System 11
2.1 CRISPR/Cas9 technology 11
2.2 CRISPR-based screens 13

3 Genome-wide Screen of Genes in the Secretory Pathway 13

4 Tribbles Pseudokinase 1 14

5 Goal 14

III Materials 15

1 Kits 15

2 Substances 15

3 Technical Devices 17

4 Buffers 17

5 Oligonucleotides 19

6 Plasmids 20

7 Cells and Bacteria 20

IV Methods 21

1 Cell Culture 21

2 Cloning 21
2.1 CRISPR/Cas9 target site cloning and sgRNA design 21
2.2 Plasmid construction 22

3 Plasmid Transformation 24

4 Transduction 24
4.1 Plasmid transfection into HEK293T lentiX cells and lentivirus production 24
4.2 Lentiviral infection of target cell lines 25

5 Puromycin Selection 25

6 Fluorescence Activated Cell Sorting (FACS) 25
  6.1 Single cell sorting and bulk sorting 25
  6.2 FACS sample preparation for CD2 analysis 26

7 DNA Analysis 26
  7.1 Genomic DNA isolation 26
  7.2 Polymerase chain reaction (PCR) 26
  7.3 PCR product cleanup 26

8 Sanger Sequencing 27

9 Confocal Imaging 27
  9.1 The Retention Using Selective Hooks (RUSH) system 28
  9.2 CD2 expressing KBM7 RUSH Cells 28
  9.3 Sample preparation for confocal imaging 29
  9.4 Assessment of confocal microscopy 29

10 RNA Analysis 30
  10.1 RNA isolation 30
  10.2 cDNA synthesis 30

11 ER Stress Assay 30

12 SDS-Polyacrylamide Gel Electrophoresis and Western Blotting 31

V Results 33

1 Targeting *TRIB1* by CRISPR/Cas9 33
  1.1 CRISPR/Cas9 target site cloning 33
  1.2 Assessment of CRISPR/Cas9 targeting 34

2 Protein Secretory Trafficking in *TRIB1* KO cell lines 36
  2.1 FACS analysis of CD2 expressing KBM7 cells 36

3 Reconstitution of *TRIB1* KO Cell Lines 37
  3.1 Vector cloning 37
  3.2 Assessment of *TRIB1* targeting and reconstitution 40

4 Effect of *TRIB1* Reconstitution on Protein Trafficking 41
  4.1 FACS analysis of *TRIB1* KO and *TRIB1* reconstituted CD2 KBM7 cells 41
  4.2 Imaging of CD2-RUSH KBM7 cells 42

5 ER Stress Response to Tunicamycin Treatment 47

VI Discussion..49

1 TRIB1 as Orchestrator of the Secretory Pathway...49

2 Determining TRIB1’s Roles..50

3 Challenges and Limitations of this Project..51

4 Conclusion and Outlook...54

VII Summary..55

VIII Table Index 57

IX Figure Index 57

X References...59

XI Appendix...67

1 Acknowledgements..67

2 Affidavit...68

I List of Abbreviation

Cas9	CRISPR associated protein 9
cDNA	Complementary deoxyribonucleicacid
CHOP	C/EBP homologous protein
CRISPR	Clustered Regularly Interspaced Short Palindromic Repeats
CTSC	Cathepsin C
DAPI	4′,6-Diamidin-2-phenylindole
DNA	Deoxyribonucleic acid
DSB	Double Strand break
EDTA	Ethylenediaminetetraacetic acid
ER	Endoplasmic reticulum
FACS	Fluorescene activated cell sorting
FBS	Fetal bovine serum
FCS	Fetal calve serum
GAPDH	Glycerinaldehyd-3-phosphatDehydrogenase
GFP	Green fluorescent protein
sgRNA	Single guide RNA
HA	Hemagglutinin
HBS	Hepes buffered saline
HEPES	2-(4-(2-Hydroxyethyl)-1-piperazinyl)- Ethansulfon acid
KO	Knockout
LB	Liquid broth
mRNA	Messenger ribonucleic acid
MFI	Mean fluorescence intensity
NT	Nontargeted
PCR	Polymerase chain reaction
qPCR	Quantitative PCR
RCF	Relative centrifugal force
RFP	Red fluorescent protein
RNA	Ribonucleic acid
rRNA	Ribosomal RNA
RT-PCR	Reverse transcription PCR
SBP	Strepavidin binding peptide
SDS-PAGE	Sodium dodecyl sulfate polyacrylamide gel electrophoresis

TE	Tris EDTA
TRIB1	Tribbles pseudokinase 1
UPR	Unfolded protein response
UV	Ultraviolet
WT	Wildtype
XBP1	X-box protein 1

II Introduction

In eukaryotic cells, most metabolic processes are compartmentalized into discrete organelles. Ever since the 1960s, cell biologists have been researching the complex processes, by which these organelles are formed, maintained and how they communicate (Bednarek & Raikhel, 1992; Rothman & Orci, 1992). Although our understanding has majorly progressed, many questions in basic cell biology including organelle interaction and protein trafficking still need to be investigated. This is especially important considering the high number and diverse subsets of diseases that are linked to dysfunctions in the secretory pathway. For instance, in class II familial hypercholesterolemia low density lipoprotein receptors fail to undergo vesicular trafficking and are degraded instead, resulting in higher cholesterol levels in the blood (Amara et al., 1992). While post-Golgi vesicular trafficking has been found to be crucial in Creutzfeld-Jacob disease and Scrapie (Uchiyama et al., 2013), endoplasmic reticulum (ER) proteostasis plays an important role in neurodegenerative diseases such as Alzheimer's disease and dementia (Hetz & Mollereau, 2014).

1 The Secretory Pathway

In most eukaryotic cells, trans-membrane and secretory proteins are transported through the ER-Golgi secretory pathway. This pathway consists of numerous organelles and transitional transport vesicles. Proteins bound for the ER-Golgi secretory pathway contain signal peptides that direct them to the ER, the entry point for most membrane-resident and soluble proteins. After specific modifications and proper folding in the ER, proteins are further transported to the Golgi apparatus. The Golgi apparatus is the central compartment for intracellular protein modification and trafficking. Upon receiving Cargos from the ER, the Golgi apparatus post-translationally processes these and sorts them (Boncompain et al., 2018; Guo et al., 2014). From there, the flow of secretory proteins is directed through the organellar system, towards their final destination (Bednarek & Raikhel, 1992; Nickel & Rabouille, 2009).

In order to ensure proper protein assembly, folding and trafficking, several mechanisms play roles for the quality control in the ER as well as in other compartments of the secretory pathway (Bukau et al., 2006; Dobson, 2003; Ellgaard & Helenius, 2003). Only after passing a stringent selection process, newly synthesized proteins are further transported to their target organelle. Aberrant products, caused by cell stress, genetic mutations or as side product of normal protein biosynthesis, are degraded and do not continue down the secretory pathway (Aridor & Hannan, 2002; Gregersen et al., 2006; Sitia & Braakman, 2003).

1.1 ER stress and homeostasis

When unfolded or misfolded proteins accumulate above a critical threshold, ER stress is invoked (Walter & Ron, 2011). In this state, a process called ER-associated degradation (ERAD) is activated by which these misfolded proteins are degraded by the proteasome (Smith et al., 2011). In order to restore cell homeostasis, the ER additionally initiates a complex signal transduction pathway referred to as the unfolded protein response (UPR), that comprises the activation of the three UPR stress sensors namely inositol-requiring protein 1 (IRE1), activating transcription factor 6 (ATF6) and protein kinase RNA-like ER kinase (PERK) by dissociation of binding immunoglobulin protein BiP (Wang & Kaufman, 2012). Through transcriptional as well as non-transcriptional effects, almost every aspect of the secretory chain is affected by UPR induction.

By phosphorylating the alpha subunit of the eukaryotic translation initiation factor 2 (eIF2a), PERK initiates a prompt attenuation of protein translation leading to a decrease of protein accumulation in the ER. Paradoxically, phosphorylated eIF2a has an enhancing effect on C/EBP homologous protein (CHOP), which itself induces protein translation (Han et al., 2013; Harding et al., 2003; Marciniak et al., 2004). At the same time, the IRE1a and ATF6 pathway both reduce ER stress by increasing ER folding and ERAD capacities. While activated IRE1a splices Xbp1 (Calfon et al., 2002), which in its spliced form induces expression of ER chaperone genes and components of ERAD (Zhang & Kaufman, 2008), ATF6a is cleaved in the Golgi apparatus and releases a fragment, that traffics to the nucleus with the same consequence (Haze et al., 1999; Wu et al., 2007).

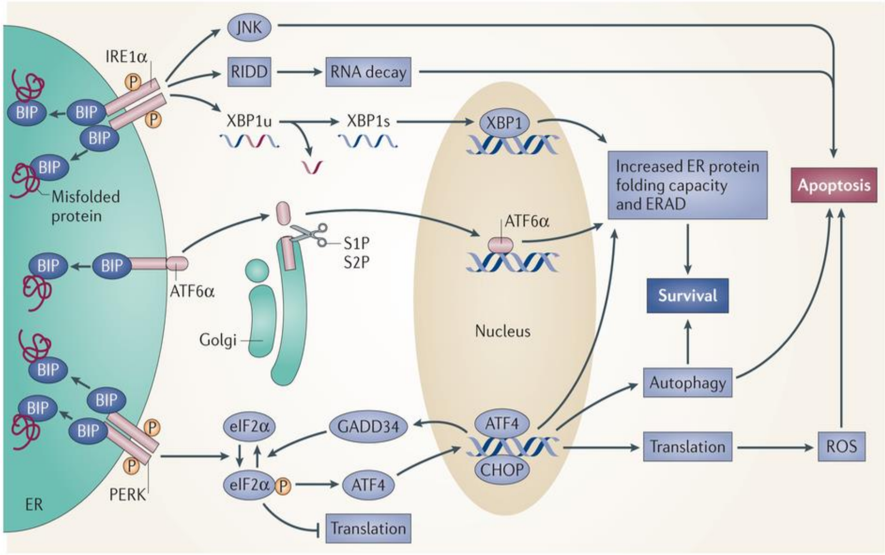
JNK
IRE1α
P
RIDD
RNA decay
BIP
XBP1u
XBP1s
XBP1
Increased ER protein folding capacity and ERAD
Apoptosis
Misfolded protein
ATF6α
S1P
S2P
Survival
Golgi
Nucleus
Autophagy
eIF2α
GADD34
ATF4
CHOP
Translation
ROS
PERK
ER

Nature Reviews | Cancer

The impact of the endoplasmic reticulum protein-folding environment on cancer development. (M. Wang & Kaufman, 2014)

1.2 The Golgi apparatus

Due to the high amount and vast variety of cargos transiting this pathway, it is not surprising that perturbations in the Golgi apparatus are involved in various human pathologies including cancer (Baschieri et al., 2015), cystic fibrosis (Park et al., 2020) and a number of neurological disorders (Van Bergen et al., 2020). Over the past few decades, it has become evident that both organized secretory trafficking and structural architecture and position of the Golgi apparatus strongly affect cell polarity, which is crucial for directed cell movement and protein secretion (Bryant et al., 2016). Previous findings also suggest that the Golgi apparatus is a highly dynamic organelle with the ability to adapt to diverse intracellular and extracellular environmental conditions (Machamer, 2015; Ravichandran et al., 2020). The architecture of the Golgi apparatus largely consists of flattened stacks of cisternal membranes, that are highly polarized and linked at the perinuclear Golgi ribbon, also called the microtubule organizing center, by tethering proteins (Barinaga-Rementeria Ramirez & Lowe, 2009; Boncompain & Perez, 2013; Klumperman, 2011; Marra et al., 2007).

However, despite extensive research, there is still no commonly accepted model explaining the mechanism of cargo-mediated transport through the Golgi (Boncompain et al., 2018). At the same time, large efforts are still required in order to provide a better understanding of the underlying pathways for Golgi homeostasis and stress response (Jansen et al., 2016; Makhoul et al., 2019). Even though the protein secretory pathway has been subject to research for decades, many questions still remain open. Applying more advanced techniques will reveal new insights into both basic mechanistic pathways of cell biology and the underlying pathology of human disease.

2 The CRISPR/Cas9 System

In the last few decades there have been numerous inventions allowing genetic modification of eukaryotic cells. One breakthrough was the discovery and bio-technological use of the clustered regularly interspaced palindromic repeats (CRISPR) and CRISPR associated protein 9 (Cas9) system. The CRISPR/Cas9 methodology enables scientists to add, alter, or delete precise locations in the mammalian DNA. Since its establishment, the CRISPR/Cas9 system has jolted numerous findings in genetic research and subsequently set a milestone in modern science (Barrangou & Doudna, 2016; Doudna & Charpentier, 2014; Fellmann et al., 2017)·.

2.1 CRISPR/Cas9 technology

The CRISPR/Cas9 gene editing technology was originally developed from the CRISPR/Cas system, an ancient immune system in prokaryotes. In this system Cas, an RNA guided endonuclease with the ability to cut double stranded DNA, plays a key role. Via a guide RNA (gRNA) consisting of 20 nucleotides the CRISPR/Cas complex is being guided to a corresponding genomic target. Upon successful binding to the target DNA the enzymatic activity of Cas results in a double strand break (DSB). Since the ultimate goal of genome editing is to target specific regions of the DNA, so called off-target binding, that may result in unwanted toxicities, is not desired.

The CRISPR/Cas9 technology was adapted from the CRISPR/Cas system in streptococcus pyogenes and is based on the same mechanism. In order to specifically increase the accuracy of complex binding and enzyme reaction in the CRISPR/Cas9 system, Cas9 will only be activated if a 3‘protospacer adjacent motif (PAM) is located next to the target sequence. The PAM motif itself must consist of three nucleotides in the order NGG with N being any base followed by two guanin bases. Only when the target sequence is directly linked to a PAM motif, Cas9 can be activated. When binding to the genomic target, Cas9 generates a DSB in the DNA, initiating cellular repair mechanisms that modify the target locus. These biological repair mechanisms are utilized to alter the genomic DNA sequence. While homology-directed repair fixes the DSB precisely according to the donor template sequence introduced into cells together with sgRNA and Cas9, the more often occurring non-homologous end joining (NHEJ) is error-prone and can cause frameshift mutations leading to loss of function mutations. The biotechnological use of this system has revolutionized the capacity to edit the genome of eukaryotic organisms (Ran et al., 2013).

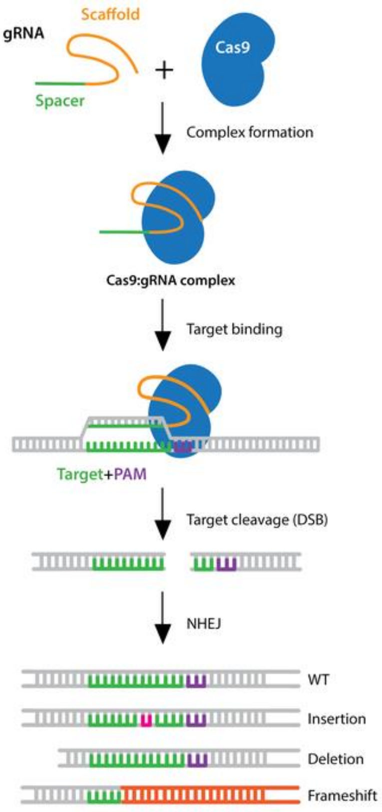

Fig. 1 CRISPR/Cas9 methodology scheme.
From CRISPR/Cas9 guide, Addgene, USA https://www.addgene.org/guides/crispr last visited 06.10.2020.

2.2 CRISPR-based screens

Genetic screens are powerful and highly efficient tools to identify and disclose relevant elements of the human genome (Shalem et al., 2015, (Koike-Yusa et al., 2014). With the establishment of the CRISPR/Cas9 technology, genetic sgRNA libraries were developed, which are capable of inducing insertion-deletion (indel) mutations in most genes of the human genome (Shalem et al., 2014; Wang et al., 2014). Using CRISPR-based screens combined with genetic sgRNA libraries, several genes or pathways have been newly identified in multiple areas of cell biology including tumor growth & metastasis or drug targeting (Fellmann et al., 2017; Kiessling et al., 2016; Parnas et al., 2015; Toledo et al., 2015). In addition, CRISPR-based screenings using the gRNA libraries targeting non-coding region of genome have contributed to explore the role of genomic sequences including enhancer elements and regulatory sequences (Korkmaz et al., 2016). Unidentified roles of the non-coding genome can be elucidated through these screenings, facilitating a more comprehensive understanding of the human genome.

3 Genome-wide Screen of Genes in the Secretory Pathway

In order to identify novel genes controlling the secretory pathway in myeloid cells, our group performed a genome-wide CRISPR/Cas9-based knockout screening. The basic idea was to unravel critical genes for the differentiation and function of myeloid cells and thus provide a new filter in the ongoing efforts to highlight novel monogenic mutations in patients with congenital neutropenia.

The next chapter addresses our screening approach and results. We performed our genome-wide, loss-of-function screen in a near-haploid, human KBM7 CML cell line (T. Wang et al., 2012). In order to track protein secretion, we engineered the cells to express CD2, a type I transmembrane protein expressed on the cell surface. Since CD2 cell surface expression is mediated by ER secretion and secretory trafficking, CD2 expression level can reflect the functionality of the secretory pathway. In our genome-wide knockout screening, CD2-expressing KBM7 cells were transduced with a lentiviral guide RNA pooled library (Addgene) including 76,441 sgRNAs targeting 19,114 human genes. sgRNAs in this library is integrated into the lentiCRISPR v2 plasmid containing a Cas9 expressing cassette and a gene conferring resistance to puromycin. After transduction, cells were selected by puromycin treatment and CD2 cell surface expression was measured by flow cytometry. Cell populations exhibiting low CD2 expression in comparison to the non-targeting sgRNA-transduced cell control as well as the whole input population were flow-sorted, and their sgRNA target regions were amplified from extracted genomic DNA by PCR, adding the flow cell attachment sequences. Purified PCR products were sequenced using next generation sequencing (NGS). The resulting sgRNA counts from each sample were analyzed using the HiTSelect algorithm, published by Dr. Aaron A. Diaz at the UCSF in 2014. We observed the algorithm ranked genes that were known to be critical for protein trafficking in the top score. Therefore, we concluded that the screen successfully provided the data set of genes related to the protein secretory pathway.

4 Tribbles Pseudokinase 1

One of the genes highly ranked in our screening results was Tribbles pseudokinase 1 (*TRIB1*). *TRIB1* is a part of the Tribbles family which consists of three protein coding genes, *TRIB1*, *TRIB2* and *TRIB3* (Eyers et al., 2017). All three proteins are pseudokinases, which indicates that they lack an ATP binding site but function similar as common kinases. TRIB1 furthermore has an N-terminal PEST region, a C-terminal MAP Kinase interaction site (Kiss-Toth et al., 2004) and a COP1 binding region (Eyers, 2015; Murphy et al., 2015). Recent studies suggest that TRIB1 is involved in protein degradation by interacting with the COP1 ubiquitin ligase (Dedhia et al., 2010). At the same time, the Trib1-COP1 complex has been shown to target CAAT Enhancer Binding Protein α (CEBPα), suggesting a role for leukemogenesis (Jin et al., 2007; Yokoyama et al., 2010).

In mice, Trib1 has been reported to control M2-like macrophage and eosinophil differentiation (Satoh et al., 2013). Recent publications suggest that Trib1 controls both eosinophil lineage commitment and neutrophil development (Mack et al., 2019). In these models, Trib1 knockout mice lacked eosinophils and showed increased numbers of neutrophils, indicating its important role in early myelopoiesis. On the other hand, Trib1 overexpression has been reported to induce acute myeloid leukemia (AML) both in mice (Dedhia et al., 2010; Yoshida, 2013) and in humans (Röthlisberger et al., 2007).

From all these studies, TRIB1 was shown to function in several pathways of high clinical relevance. However, the detailed mechanisms are yet to be identified. Elucidation of the genetic and molecular function of *TRIB1* in protein trafficking and organelle integrity might not only answer basic questions about its cellular functions but offer new opportunities for drug targeting of human diseases known to be related to TRIB1 deficiency.

5 Goal

The protein secretory pathway is a crucial part of cell biology, which is mediating both homeostasis and pathology. By applying a large-scale genome-based approach, we were able to gain a non-biased insight of genes involved in this pathway. This project therefore aims at:

1. Validation of the screen result by knocking out *TRIB1* on a CRISPR-Cas9 based method
2. Exploring TRIB1 function within the secretory pathway by tracking CD2 trafficking in *TRIB1* knockout cells

III Materials

1 Kits

Tab. 1 Kits

Kit	**Supplier**
High-Capacity cDNA Reverse Transcription Kit	ThermoFischer
illustra ExoProStar Enzymatic PCR and Sequence Reaction Clean Up Kit	GE Healthcare
NEB PCR Cloning Kit	NEB
Qiagen Maxiprep Kit	Qiagen
QIAquick Gel Extraction Kit (250)	Qiagen
RNEasy Plus Mini Kit (250)	Qiagen

2 Substances

Tab. 2 Substances

Substance	**Supplier**
2-Mercaptoethanol	Applichem
2-Propanol	Applichem
Acetone	Applichem
Agarose Basic	Applichem
Alexa Fluor 568 Anti-Rabbit Ab	Life technologies
Alexa Fluor 633 Anti-Mouse Ab	Life technologies
Ammonium Persulfate (APS)	Sigma-Aldrich
Ampicillin sodium salt	Applichem
Biotin	Sigma-Aldrich
BlueRay Prestained Protein Marker	Jena Bioscience
Bovine Serum Albumin (BSA)	Applichem
Bromophenol sodium salt	Roth
Calnexin polyclonal antibody	Enzo Life Sciences
Cell lysis buffer	Life technologies
Chloroquine diphosphate salt	Sigma-Aldrich

Dako fluorescent mounting medium	Dako
DAPI (4‘,6‘-Diamidin-2-phenylindole)	Sigma-Aldrich
dNTPs	Thermo Fischer Scientific
Dulbecco’s Modified Eagle Medium (DMEM)	Thermo Fischer (Gibco)
Dulbecco's phosphate-buffered saline (DPBS)	Thermo Fischer (Gibco)
Ethanol	Roth
Ethidium bromide	Applichem
Fast AP	Thermo Fischer Scientific
Fast Digest EcoRI	Thermo Fischer Scientific
Fast Digest Mlu1	Thermo Fischer Scientific
Fast Digest SfaAI	Thermo Fischer Scientific
Fetal Bovine Serum (FBS)	Life technologies
HEPES buffered saline	Sigma-Aldrich
Hepes buffered solution	Thermo Fischer
Hexadimethrine bromide	Sigma-Aldrich
Iscove’s Modified Dulbecco’s Medium (IMDM)	Thermo Fischer (Gibco)
Liquid Broth (LB) medium	Carl Roth
Loading Dye (6x)	Thermo Fischer Scientific
Lysis buffer	Cell Signaling
Methanol	Roth
Midrange DNA ladder	Jena Bioscience
Milk Powder	Roth
NP-40	Calbiochem
OneTaq Quick-Load 2X Master Mix with Standard Buffer	NEB
Paraformaldehyde (PFA)	Sigma Aldrich
Penicillin/ Streptomycin	Thermo Fischer (Gibco)
Phenylmethanesulfonyl fluoride (PMSF)	Alpha Diagnostic Intl
Protease Inhibitor Cocktail (PIC)	Sigma Aldrich
Puromycin	Invitrogen
Q5® High-Fidelity DNA Polymerase	NEB

Riboblock RNAse inhibitor	Thermo Fischer
Rotiphorese 30% Acrylamid	Carl Roth
RPMI+, Glutamate Supplement	Thermo Fischer (Gibco)
Saponin	Carl-Roth
Sodium Dodecyl Sulfate (SDS)	Roth
Sodium Pyruvate	Thermo Fischer
T4 DNA Ligase	Promega
Tetramethylethylenediamine (TEMED)	Carl Roth
Tris Base	Roth
Trypsin ETDA	Sigma
Tunicamycin	Sigma-Aldrich
Tween-20	Sigma-Aldrich

3 Technical Devices

Technical devices are listed under section IV appropriately.

4 Buffers

Tab. 3 Buffers

Name	**Composition**
Blocking and Permeabilization Buffer (Immunofluorescence)	5% BSA 0.05% Saponin PBS
FACS buffer	2.5% FCS PBS
Laemmli buffer (6x)	12% SDS 60% Glycerol 0.5 M Tris (pH 6,8) 0.004% Bromphenole dH_2O
Lysis buffer	835 µl Nuclease-free H_2O 100 µl 10x Lysis buffer 60 µl Protease Inhibitor 5 µl PMSF

PBS	
PBST	1x PBS 0.1% Tween-20
RIPA buffer	150 mM NaCl 1% NP-40 0.5% Sodium deoxycholate 0.1% SDS 50 mM Tris (pH 8,0) 1x Protease Inhibitor dH_2O
Running buffer (10x)	250 mM Tris Base 35 mM SDS 1.92 M Glycine dH_2O
Transfer buffer (10x)	250 mM Tris Base 1.92 M Glycine dH_2O
Tris-HCl buffer 0,5 M pH 6,8	4.7 g Tris Base dH_2O pH adjusted using Tris-HCl
Tris-HCl buffer 1,5 M (pH 8,8)	36.9 g Tris-HCl 153.9 g Tris Base dH_2O

5 Oligonucleotides

All Oligonucleotides and Primers were designed using the PrimerBlast software and purchased from Eurofins Genomics.

Tab. 4 CRISPR/Cas9 guide sequences

Target [5‘ → 3‘]	**Top strand [5‘ → 3‘]**	**Bottom strand [5‘ → 3‘]**
Target 1 AATCTGCTTGAAGAGCCGGG	CACCGAATCTGCTTGAAGAGCCGGG	AAACCCCGGCTCTTCAAGCAGATTC
Target 2 CGGAGGGCTCCCGTCTCAAG	CACCGCGGAGGGCTCCCGTCTCAAG	AAACCTTGAGACGGGAGCCCTCCG

Tab. 5 Primers for seqencing

Primer	**Sequence [5‘ → 3‘]**
LKO.1 5‘ f	GACTATCATATGCTTACCGT
pMini f	ACCTGCCAACCAAAGCGAGAAC
pMini r	TCAGGGTTATTGTCTCATGAGCG

Tab. 6 Primers for cloning

MluI-TRIB1 f	attacgcgtATGCGGGTCGGTCCG
TRIB1-SfaAI r	gtagcgatcgcGCAGAAGAAGGAACT

Tab. 7 Primers for genome check

Primer	**Sequence [5‘ → 3‘]**
TRIB1 f1	GGACAAAATCAGGCCTTACATC
TRIB1 r1	AACTTCCTAAGCTTCAGGTCCC
TRIB1 f2	CTCTACACCCTTCTGGTTGGAC
TRIB1 r2	TGTCCTCCTGGTACTCTGGAAC

Tab. 8 Primers for RT-PCR

Primer	**Sequence [5‘ → 3‘]**
CHOP f	ATGAACGGCTCAAGCAGGAA
CHOP r	GGGAAAGGTGGGTAGTGTGG
GAPDH f	GTGGGGCGCCCCAGGCACCA
GAPDH r	CTCCTTAATGTCACGCACGATTTC
TRIB1 mRNA f1	GAAGAGGCTGCGGGAAGAG
TRIB1 mRNA r1	CTGGGTTCTCTCCTCCGTG
TRIB1-mRNA f2	AGAGAACCCAGCTTAGACTAGA
TRIB1-mRNA r2	AGGCTCCAAACGTCCGC
TRIB1-mRNA f3	CCACCAGTCAGCCATCGT
TRIB1-mRNA r3	TCCCAGTGGTGTTGAGGATC
XBP1-s f	TTACGAGAAAACTCATGGC
XBP1-s r	GGGTCCAAGTTGTCCAGAATG

6 Plasmids

Tab. 9 Plasmids

lentiCRISPRv2	Addgene (Zhang Lab)
pMiniT2.0 vector	New England Biolabs
pRRL IRES-RFP	Addgene
TRIB1 ORF in pcDNA3.1+	Genescript

7 Cells and Bacteria

Tab. 10 Cell lines and bacteria strains

HEK293T lenti-X™ Cell Line	Takara Bio
KBM7 cell line	Horizon Discovery
XL10Gold *E.coli*	Agilent

IV Methods

1 Cell Culture

Adherent 293T cells were cultivated in DMEM supplemented with 10% fetal calf serum (FCS), 2 mM L-glutamine, 50 U/ml penicillin and 50 µg/ml streptomycin. Trypsin-EDTA was used to dissolve the adherent cells for cell splitting. Non-adherent KBM7 cells were cultured in IMDM with the same supplements. The substances added to the medium are important for cell growth and reproduction. FCS contains proteins, hormones and lipids that promote cell growth and division. The antibiotics penicillin and streptomycin are used to prevent contamination of the cell cultures with their combined action against gram-positive and gram-negative bacteria. Cells were split every two to three days and cultivated in an incubator at 37 °C, 95% humidity and 5% CO2.

2 Cloning

2.1 CRISPR/Cas9 target site cloning and sgRNA design

The target site was chosen using the software CHOPCHOP (https://chopchop.cbu.uib.no/) under consideration of known characteristics and functions of the gene such as active domains and number of exons displayed on Ensembl (m.ensembl.org) and Uniprot (www.uniprot.org). Corresponding sgRNA strands were designed and purchased as indicated in Tab. 4.

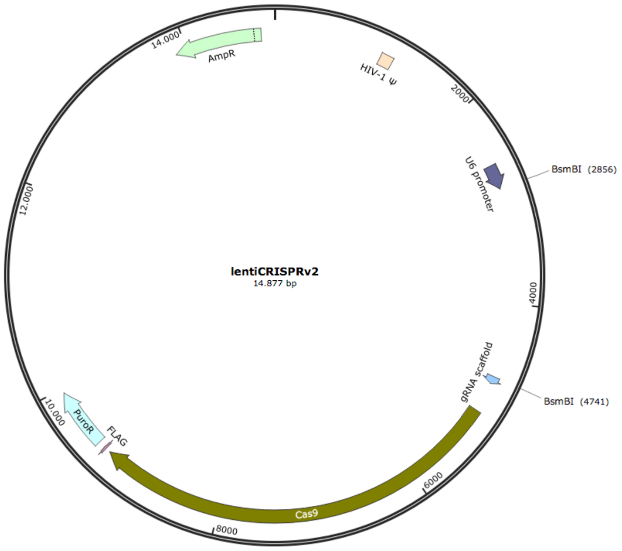

Fig. 2 LentiCRISPRv2 vector. Restriction sites for BsmBI. Map made with SnapGene

2.2 Plasmid construction

Target guide sequences were cloned into the lentiCRISPRv2 vector. This plasmid contains Cas9, as well as Puromycin (Puro) and Ampicillin (Amp) resistant genes. The lentiCRISPRv2 plasmid was digested with the restriction enzyme BsmBI for 30 min at 37 °C and dephosphorylated with Fast AP for 15 min at 37°C. The size of the digested plasmid was confirmed by electrophoresis on a 1% agarose gel for 40 min at 120 mV and the DNA was purified from the gel using the Qiaquick Gel extraction kit according to the manufacturer’s protocol. Hereby the gel slice containing the DNA band was excised using a sharp scalpel, diffused with buffer and incubated at 50° C for 30 min. After centrifugation, the supernatant containing the DNA was passed through a filter in order to remove residual polyacrylamide gel. The extracted DNA was then bound to a column by centrifugation, washed several times using different buffers and finally yielded using elution buffer. Thereupon the top and bottom strands of the sgRNA were annealed, phosphorylated by T4 polynucleotide kinase and ligated into the lentiCRISPRv2 vector using the T4 DNA ligase according to the manufacturer’s protocol.

For *TRIB1* reconstitution, human *TRIB1* complementary DNA Open Reading Frame (ORF) clone was obtained from Genescript and digested using the restriction enzymes BamHI and BclI. Successful cutting was confirmed by electrophoresis on a 1% agarose gel and DNA fragment with the correct size was extracted from the gel using the Qiaquick Gel extraction kit mentioned in the paragraph above. Subsequently the *TRIB1* sequence was amplified via Q5 High Fidelty PCR using primers designed with overhangs for the restriction sites MluI and SfaAI in the forward primer and the reverse primer (Primer: MluI-TRIB1 f, TRIB1-SfaAI r), respectively. The PCR product was subjected to electrophoresis on a 1% agarose gel and the DNA was extracted using the Qiaquick Gel extraction kit. Since direct ligation into the lentiviral vector was not successful, the MluI-kozak-TRIB1-SfaAI amplicon was first cloned into the

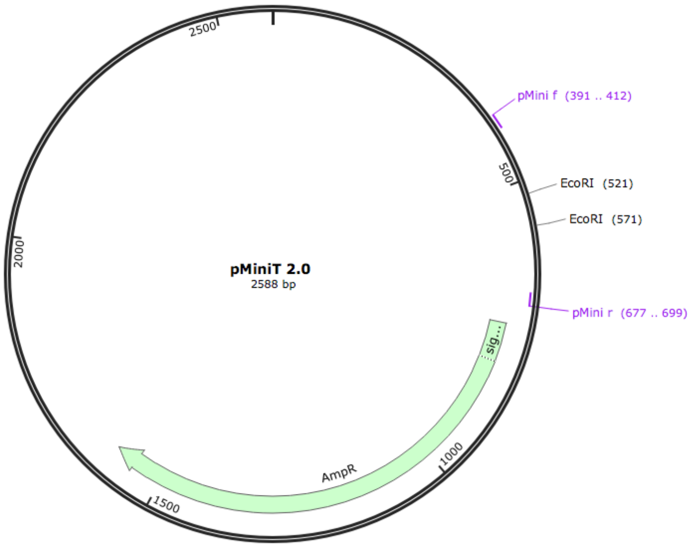

Fig. 3 pMiniT2.0 cloning vector. Primers for cloning check pMini f and pMini r. EcoRI restriction site. Map made with SnapGene.

pMiniT2.0 cloning vector by blunt end ligation using the T4 DNA ligase. The constructed plasmid was transformed into *E.coli* for further growth and obtained from the bacteria via Miniprep on the next morning (see 2 Plasmid Transformation). Subsequently the MluI-TRIB1-SfaAI-pMiniT2.0 plasmid was digested and dephosphorylated with the restriction enzyme EcoRI for 30 min at 37 °C. The digestion product was separated via electrophoresis on a 1% agarose gel size check of the insert. After size confirmation via vector digestion the correct insertion into the pMiniT2.0 plasmid was rechecked via Sanger sequencing using the pMini f and the pMini r primers and the SeqMan Pro software. The MluI-TRIB1-SfaAI-pMiniT2.0 vector was then digested using the restriction enzymes MluI and SfaAI for 30 min at 37 °C, subjected to electrophoresis on a 1% agarose gel. The DNA fragment of approximately 1.2 kb, corresponding to the length of MluI-TRIB1-SfaAI amplicon, was extracted from the gel using the Qiaquick Gel extraction kit. Subsequently the MluI-TRIB1-SfaAI amplicon was cloned into the pRRL lentiviral vector harboring IRES-RFP cassette downstream of the insertion site.

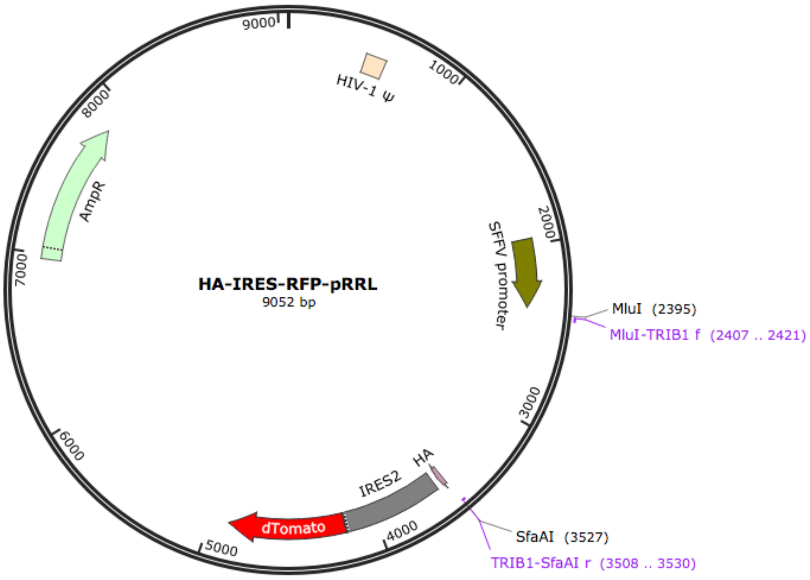

Fig. 4 HA-IRES-RFP-pRRL lentiviral vector. Primers for cloning check (MluI-TRIB1 f, TRIB1-SfaAI r). Restriction sites MluI and SfaAI. Map made with SnapGene

Therefore, the HA-IRES-RFP-pRRL vector was digested using the restriction enzymes MluI and SfaAI for 30 min at 37 °C, size checked via electrophoresis on a 1% agarose gel and extracted from the gel using the Qiaquick Gel extraction kit. Using the T4 DNA Ligase the MluI-TRIB1-SfaAI amplicon was ligated into the pRRL lentiviral vector. The proper insertion of MluI-TRIB1-SfaAI was confirmed by Sanger sequencing using the pRRL for and IRES rev primer and subsequent check in the SeqMan Pro software.

3 Plasmid Transformation

The cloned vector was transformed into XL10Gold competent *E. coli* using the heat shock method: After suspending the plasmid with *E. coli*, a sudden increase in temperature to 42 °C for 30 sec creates pores in the bacterial cell membrane, which enables the plasmid to enter into the bacteria. The transformation product was then spread on a LB agar plate containing Amp (100 µg/ml) and incubated at 37 °C overnight. On the next morning single bacteria colonies were picked, transferred into 600 µl of LB containing Amp (100 µg/ml) and incubated at 37 °C overnight for further expansion. On the next day the plasmid was obtained from *E. coli* via Miniprep. This procedure is suited to purify up to 20 µg of plasmid DNA from bacteria and is based on alkaline lysis of bacterial cells followed by adsorption of DNA onto a silica membrane in the presence of high salt. During this process RNA, proteins, dyes, and low-molecular–weight impurities are removed by several washing steps. The correct DNA sequence of the yielded plasmids was confirmed via Sanger sequencing and subsequent sequence check using the SeqMan Pro software. *E. coli* colonies inheriting the correct plasmid were inoculated in 100 ml of LB with Amp (100 µg/ml) at 37 °C overnight for further plasmid expansion. On the next morning, enriched plasmids were extracted using Maxiprep, allowing a yield of up to 500 µg of plasmid DNA. The plasmid concentration was measured via NanoDrop 2000 spectrophotometer with an amount of 2-10 µg/µl in average and subsequently diluted down to 1 µg/µl for plasmid transduction.

4 Transduction

After vector cloning and transformation, the plasmid was transduced into the target cell lines.

4.1 Plasmid transfection into HEK293T lentiX cells and lentivirus production

For transfection, HEK293T lentiX cells were seeded in 6-well plates at a density of $1x10^4$ cells/ml one day prior transfection. Shortly before transfection, the culture medium was changed into DMEM supplemented with 10 mM HEPES, 1 mM Sodiumpyruvate and 25 µM Chloroquine. Thereupon the lentiviral plasmids were transfected into HEK293T lentiX cells at 70% confluence together with the lentiviral packaging vector psPAX2 and the envelope vector pMD2.G by calcium phosphate method. The plasmids were suspended in a 1: 2: 5 ratio (pMD2.G: psPAX2: lentiCRISPRv2) in calcium chloride (0.125 M in final) and low Tris EDTA first, mixed with 2x HBS by bubbling air through HBS and incubated for 30 min at room temperature. In this way plasmid DNA can bind to calcium phosphate and enter the cells by endocytosis. After incubation, the plasmid solution was added to the HEK293T lentiX cells and the cells were incubated at 37 °C for 8-12 h. The medium was replaced by IMDM supplemented with 10% FBS and Penicillin/ Streptomycin (P/S). 72 h after transfection, I harvested the supernatant containing the secreted lentivirus, centrifuged it at 850 RCF for

30 min at 4 °C and passed it through a 0.45 µm filter. The virus was either immediately used for cell infection or stored at -80 °C.

4.2 Lentiviral infection of target cell lines

One day prior infection, CD2 expressing KBM7 cells and CD2 expressing KBM7 RUSH cells were seeded in 24-well plates at a density of 1x10^5 cells/ml. On the next day, target cells were collected and diluted in IMDM medium containing 0.05% Hexadimethrine bromide, a cationic polymer widely used to increase transduction efficiency in cell culture. Previously produced lentivirus was added to the cell suspension and subjected spin infection at 400 RCF for 60 min at 37 °C. Fresh medium was added followed by an incubation period of 5-11 h. Infected cells were then resuspended with fresh culture medium, transferred into new plates and incubated for 2-3 days.

5 Puromycin Selection

After lentiCRISPRv2 transduction, Puromycin (1µg/ml) was added and cells were cultured for 3-6 days. During this incubation period only successfully transduced cells, that harbor a vector containing a Puromycin resistant site expand.

6 Fluorescence Activated Cell Sorting (FACS)

In this project, FACS was used to measure CD2 expression on the cell surface. During this procedure, cells individually pass through a capillary and are stimulated by a laser beam. Meanwhile the resulting scattered light or possible fluorescent light is detected. The amount of light scattered by the cell correlates with, among other things, its size, which can be read in the intensity of the forward scattered light (Forward Scatter, FSC). In order to define the characteristics of the sorted cells, the FACSDiva software was used, which displays the measured data in a scatter plot or histogram.

6.1 Single cell sorting and bulk sorting

Following Puromycin selection in lentiCRISPRv2 transduced target cells and 2-3 days after HA-IRES-RFP-pRRL transduction, successfully transduced cells were selected using the FACSAria machine. Therefore, cells were collected by centrifugation and resuspended in FACS buffer. Shortly prior to sorting the cell suspension was transferred into FACS tubes with blue filter caps and stored on ice throughout the sorting process.

LentiCRISPRv2 transduced cells were single cell sorted into 96-well plates containing 200 µl of culture medium based on viability. Cells were incubated for 3 weeks or more and observed weekly. Single cell clones indicating macroscopic growth were transferred into 24-well plates for further expansion.

HA-IRES-RFP-pRRL transduced cells were sorted based on RFP expression. Cells with high expression level of RFP were collected in a 15 ml Falcon and transferred into T25 flasks containing 7 ml of culture medium after sorting. Cells were incubated for further expansion.

6.2 FACS sample preparation for CD2 analysis

About $1x10^6$ cells were stained with Phycoerythrin (PE) conjugated anti-CD2 Antibody (Ab) or Pacific Blue conjugated anti-CD2 Ab. Therefore, cells were collected and washed with FACS buffer. Antibodies were diluted (1:250 for PE, 1:200 for Pacific Blue) in FACS buffer, suspended with the cell samples and incubated for 1 h in the dark at room temperature. After that, cells were washed twice with FACS buffer and transferred through a FACS tube with a filter cap. By passing through the incorporated 25 µm Nylon mesh, residual antibody and large waste particles are removed fabricating a more purified cell lysate. The intensity of PE or Pacific Blue fluorescence was measured by the LSR Fortessa cell analyzer. FACS results were analyzed using the FlowJo software.

7 DNA Analysis

7.1 Genomic DNA isolation

In order to check CRISPR targeting effects on the genomic level, genomic DNA was isolated. Therefore, about $1x10^6$ cells were collected by centrifugation at 800 RCF for 3 min. The cell pellet was resuspended with 50 mM NaOH in elution buffer, boiled for 15 min at 95 °C and neutralized using 1M Tris Buffer (pH= 7.0). DNA yielded in this process built the template for the subsequent genome check and was stored at 4 °C.

7.2 Polymerase chain reaction (PCR)

Polymerase chain reaction in combination with specific primer sets was used in various stages of this project under diverse conditions indicated in each Figure individually. An Agarose gel run including DNA ladders followed by visualization via UV illumination indicated PCR products and DNA sizes.

7.3 PCR product cleanup

Small nucleotides and primers perturbing sequencing results were destroyed using ExoSAP-IT^{TM} following the manufacturer's manual. The PCR product was sequenced using forward primers for the PCR.

8 Sanger Sequencing

Sanger sequencing, also called the Sanger dideoxy method, facilitated the assessment of individual DNA fragments in a targeted manner. This process is based on the principle of the chain termination method, in which the polymerization reaction is terminated by using dideoxynucleoside triphosphates (ddNTPs). According to the old method, four reactions, each with a radioactively labeled ddNTP, are set up and the PCR products are then separated and analyzed by gel electrophoresis. A newer method is based on a single approach, in which all four ddNTPs are coupled with different fluorescent dyes. The resulting chain termination products are separated using capillary electrophoresis and subsequently analyzed using their different fluorescent colors (Shendure, Porreca et al. 2011, Park and Kim 2016).

In this project, Sanger sequencing results were analyzed using the SeqMan Pro software. Therefore, Sanger sequences were assembled with the reference DNA sequence from Uniprot (www.uniprot.org). For CRISPR targeting assessment, indel mutations at the target locus in the *TRIB1* genome were detected by SeqMan Pro and individually investigated.

9 Confocal Imaging

Confocal imaging is a microscopy-based method, that allows tissue or cell imaging with a high quality of optical resolution. The confocal microscope is named according to its special technical features: In contrast to wide field microscopes the confocal microscope uses point illumination, when detecting fluorescence. This means that only a specific part – instead of the whole slide – is illuminated. Additionally, the sample’s fluorescence has to pass through a pinhole before reaching the detector, so only the in-focus fluorescence is being detected. By using oscillating mirrors, the light beam is scanned through the specimen in a regular raster. These successive slices are then stacked together to build a 2D or 3D image of the sample. All of these mechanisms together result in a very high optical resolution of the image. Since a high percentage of the sample’s fluorescence is blocked at the pinhole (the so-called out-of-focus light), longer exposure time is required to higher the fluorescence’s intensity. The in-focus fluorescence is then transformed into an electrical signal and analyzed by a computer software. We used the ZEISS Laser scanning Microscope 800 for confocal imaging.

9.1 The Retention Using Selective Hooks (RUSH) system

The Retention using selective hooks system is a tool to observe protein secretory trafficking (Boncompain et al., 2012). In the RUSH system a hook protein is reversibly fused to core streptavidin. Both are stably anchored in the donor compartment, whereas the protein of interest is fused to streptavidin binding peptide (SBP). Upon Biotin addition to the cells, the protein of interest is synchronously released from the hook protein and starts trafficking to its final compartment. In order to observe this process via microscopy, the protein of interest can be fused to a fluorescent protein, which is then detected via confocal imaging. In order to focus on the protein trafficking itself without the influence of overall CD2 expression by reduced transcription or translation, we established a KBM7 cell line inheriting the RUSH system with a CD2 reporter protein. In our CD2-RUSH system, the GFP fused CD2 is retained in the ER by an interaction between the SBP in the N-terminal of GFP-CD2 and Streptavidin in the hook protein, which is ER resident due to the KDEL sequence.

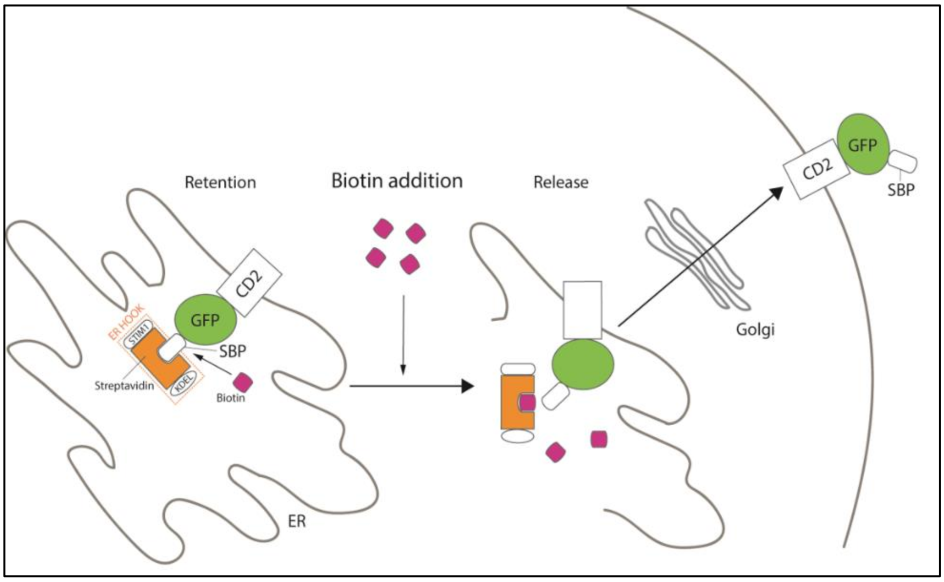

Fig. 5 Retention using selective hooks (RUSH) system in GFP tagged CD2 KBM7 RUSH cells. The Hook is stably anchored in the ER, while GFP tagged CD2 is reversibly fused to Streptavidin via SBP. Biotin addition releases SBP from the hook. which enables GFP tagged CD2 to start trafficking. ER, endoplasmic Reticulum. GFP, Green fluorescent Protein. SBP, Streptavidin binding peptide. CD2, Cluster of Differentiation 2. Figure made with Adobe Illustrator.

9.2 CD2 expressing KBM7 RUSH Cells

KBM7 cells were transduced with the CD2-RUSH-pRRL plasmid containing an ER hook, Streptavidin binding peptide (SBP) and GFP tagged CD2. These CD2 KBM7 RUSH cells were used for tracking of intracellular CD2 trafficking.

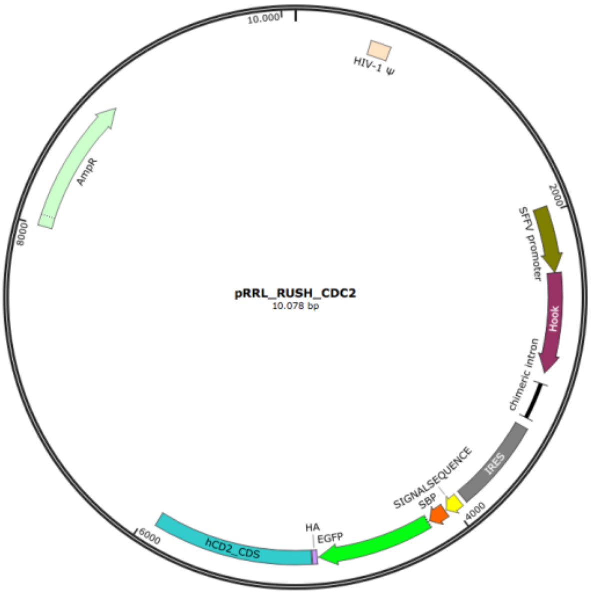

Fig. 6 CD2-RUSH-pRRL vector for KBM7 cell transduction. GFP tagged CD2-RUSH transduced KBM7 cells were provided by Dr. Megumi Tatematsu. The vector was liberally provided by Drs. Michael Braun and Julia von Blume.

9.3 Sample preparation for confocal imaging

$1x10^5$ CD2 KBM7 RUSH cells were collected and 40 µM Biotin was added at different time points. Cells were fixed by 4% PFA for 15 min, washed and permeabilized with 0.1% Saponin in 1% BSA-PBS. The Golgi apparatus was stained with anti-GM130 Ab (1:250 dilution) and the endoplasmic reticulum was stained with anti-Calnexin Ab (1:200 dilution) for 60 min at room temperature. After washing, cells were stained with secondary fluorescent antibody for 45 min at room temperature in the dark. After washing and resuspending in PBS, cells were transferred on the slide glass by cytospin at 500 rpm for 5 min. Samples were sealed with mounting media containing DAPI staining for the nucleus and a cover glass. Imaging slides were stored at room temperature in the dark.

9.4 Assessment of confocal microscopy

CD2 trafficking was imaged using a 96x oil objective in a ZEISS Laser scanning Microscope 800 with four different lasers and visualized by the ZEN2.0 software. Imaging configurations were standardized for all samples and master gain as well as laser power settings were only minimally adjusted to differing imaging conditions for comparability.

10 RNA Analysis

10.1 RNA isolation

RNA was isolated using the RNEasy Plus Mini Kit according to the manufacturer's instructions. The RLT buffer in which the cells were initially lysed contains guanidine isothiocyanate and 2-Mercaptoethanol to inactivate RNases. The addition of ethanol creates conditions in which the RNA binds to a silica membrane present in the column. After repeated washing, RNA was eluted from the column using RNase-free water. The concentration and quality of the isolated RNA was measured using NanoDrop spectrophotometer. The RNA suspension was subsequently diluted to 1000 ng/µl and stored at -70 °C.

10.2 cDNA synthesis

Isolated RNA was reverse transcribed using the High-Capacity cDNA Reverse Transcription Kit. For each reaction 1000 ng RNA, 2 µl 10x RT Puffer, 0,8 µl 25x dNTP Mix (100 mM), 2 µl 10x RT Random Primer, 1 µl MultiScribe^{TM} Reverse Transcriptase and NF H2O were used at a total scale of 20 µl per reaction under the following cycling conditions:

Step 1:	10 min at 25°C
Step 2:	120 min at 37°C
Step 3:	5 min at 85°C
Step 4:	Storage at 4°C

11 ER Stress Assay

Tunicamycin is an antibiotic which is naturally produced by several Streptomyces and inhibits the synthesis of N-linked glycoproteins by blocking the initial step of glycoprotein synthesis species (Reiling et al., 2011). In this way it causes the accumulation of misfolded or unfolded proteins in the ER subsequently disturbing ER homeostasis. This pharmacological approach enables a strong and specific UPR induction in a short time period (Han & Kaufman, 2014). About $1x10^6$ of CD2 expressing KBM7 cells were cultured in medium containing 2 µg/ml Tunicamycin for 2 h or 8 h. Controls were not subjected to Tunicamycin treatment and labelled as 0 h. RNA was extracted using the RNEasy Plus Mini Kit according to the manufacturer’s instructions. RNA concentration and quality were measured by Nanodrop spectrophotometer and diluted to 1000 ng/µl. RNA was transcribed to cDNA using the High-Capacity cDNA Reverse Transcription Kit as described in 10.2. Induction of ER stress response genes was assessed by PCR with Onetaq polymerase using according primers (Tab. 8) and subsequent gel electrophoresis.

12 SDS-Polyacrylamide Gel Electrophoresis and Western Blotting

SDS-polyacrylamide gel electrophoresis (SDS-PAGE) facilitates the separation of proteins according to their molecular weight. The separated proteins are then transferred from the gel to a polyvinylidene difluoride (PVDF) membrane by Western blotting and are subsequently detected by antibodies.

For protein extraction, cells were collected and resuspended with a mixture of nuclease free water and lysis buffer supplemented with protease inhibitor Phenylmethylsulfonylfluoride (PMSF). After incubation on ice for 15 min, the cell lysate was subjected to centrifugation at 18,000 RCF for 10 min at 4 °C. The supernatant was mixed with Laemmli buffer supplemented with 2-Mercaptoethanol (2-ME) and boiled for 5 min at 95 °C. Subsequently the protein was resolved by SDS-PAGE run at 80-120 mV for 2 h.

Tab. 11 Components of running and stacking gel for SDS-PAGE

Running gel (10%)	**Stacking gel (5%)**
4 ml NF H_2O	2 ml NF H_2O
3.3 ml Acrylamide	487.5 µl Acrylamide
2.5 ml Tris-HCl (1.5 M, pH 8.8)	360 µl Tris-HCl (0.5 M, pH 6.8)
0.1 ml SDS (10%)	28.75 µl SDS (10%)
50 µl APS	18.75 µl aps (20%)
4 µl TEMED	2.075 µl TEMED

The gel was then transferred onto PVDF membrane (Roth) at 4°C at 400 mA for 90 min in a Tank-Blot-System (Bio-Rad). After blocking in 5 % skim milk for 60 min, the membrane was incubated in 1% BSA containing 1:500 diluted anti-TRIB1 Ab, 1:1000 diluted anti-HA Ab, 1:1000 anti-CTSC Ab overnight. Following several washing steps with PBS-T (3x10 min) the membrane was incubated with HRP-conjugated secondary Abs in 2.5% skim milk for 60 min at room temperature under gentle shaking. After another washing step, proteins were detected using chemiluminescence reagent combined with the chemiDoc XRS+ Imaging System (Bio-Rad). Western blots were analyzed and quantified using the ImageLab software.

V Results

TRIB1 knockout cell lines were established via CRISPR/Cas9 targeting and CD2 trafficking was observed in order to show, whether

1) TRIB1 might play a role in protein trafficking as indicated by the former performed genome wide knockout screening,
2) at which stage protein secretory trafficking might be perturbed and whether
3) protein trafficking can be restored upon *TRIB1* reconstitution.

1 Targeting *TRIB1* by CRISPR/Cas9

1.1 CRISPR/Cas9 target site cloning

In order to create TRIB1-deficient cells, we targeted a genomic locus close to the protein's active domain. According to previous findings (Kiss-Toth et al. 2004, Qi et al. 2006, Dehia et al. 2010), the C-terminus of Trib1 plays an important role for several intracellular pathways such as COP1 and MAPK binding. We identified the exact region of the protein interaction domain using UniProtKB (https://www.uniprot.org) to be at the amino acid positions 351-372 in exon 3 and decided to target an area before this critical region.

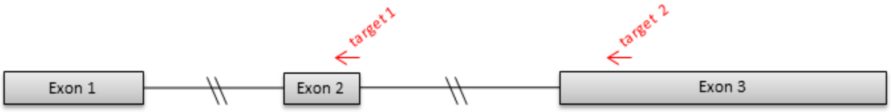

Fig. 7 *TRIB1* gene. Total of three exons, intronic sequences are shortened. Red arrows indicate approximate target region of sgRNA1 and sgRNA2

We constructed a lentiCRISPRv2 plasmid containing the corresponding sgRNA and transduced it into CD2 expressing KBM7 cells and CD2 expressing KBM7 RUSH cells.

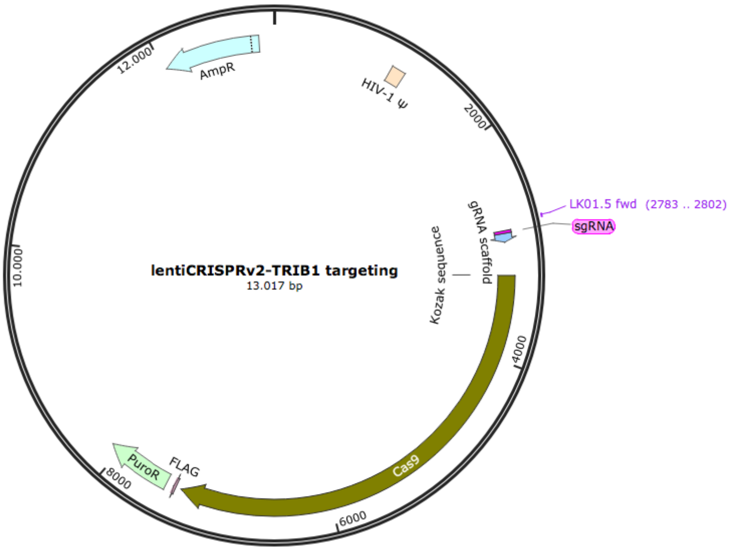

Fig. 8 Constructed lentiCRISPRv2 vector for *TRIB1* targeting. sgRNA top and bottom strands were annealed and ligated into the digested lentiCRISPRv2 vector. The correct construction was confirmed via sequencing using the Primer LKO1.5' fwd. The vector map was created with SnapGene. AmpR, Ampicillin resistance. PuroR, Puromycin resistance. HIV-1, human immunodeficiency virus 1.

Since the backbone of the lentiCRISPRv2 plasmid contains a puromycin resistant site, I was able to generate a population of successfully transduced cells by puromycin selection. As repaired sequence by NHEJ upon double strand break vary from cell to cell, we generated different *TRIB1* targeted cell lines by single cell sorting using FACSAria.

1.2 Assessment of CRISPR/Cas9 targeting

In order to analyze the effect of CRISPR/Cas9 editing of the TRIB1 locus, we isolated DNA of transduced single cell clones and amplified the target sequence via PCR using genome specific primers (Tab. 5).

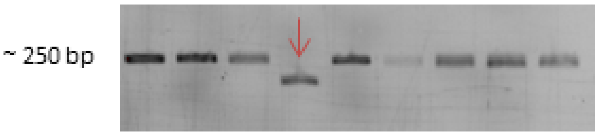

Fig. 9 Exemplary PCR of *TRIB1* target locus in different single cell clones using Onetaq Polymerase. The *TRIB1* target locus was amplified using a specific primer set for genome check with an intended product size of 274 bps. The PCR product was subjected to an agarose gel run on 1.5 % agarose and visualized using the ImageLab software. The red arrow indicates one single cell clone with base deletions in the target locus already detectable by PCR.

The amplified target locus was then sequenced and manually compared to the *TRIB1* reference genome using the software SeqMan Pro. Base deletions, that were a number of 3 or a multiple of 3 were disregarded, because these mutations rather result in amino acid deletions, than in frameshift mutations with following loss of protein function.

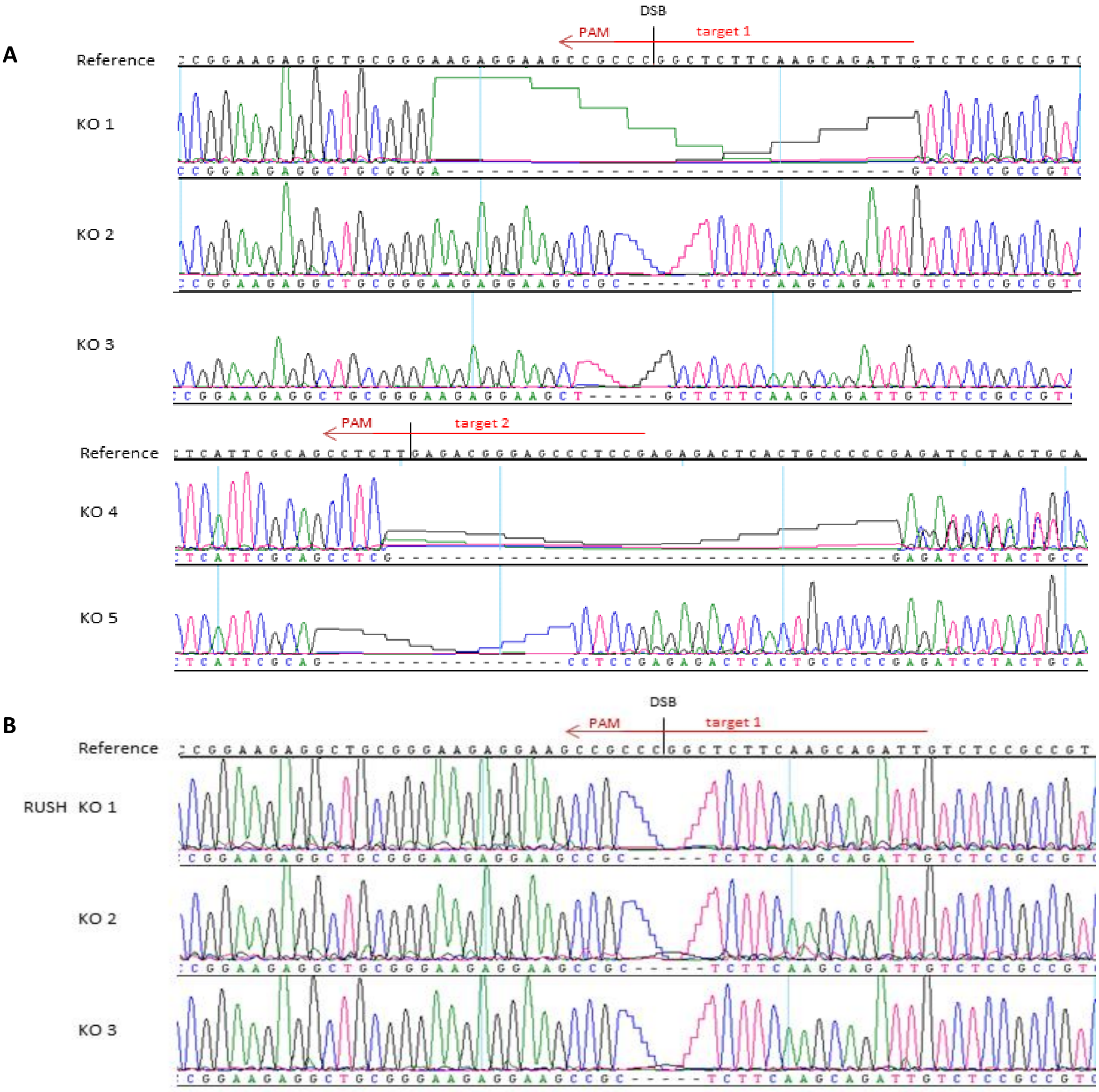

Fig. 10 Chromatogram of *TRIB1* target locus in lentiCRISPRv2-TRIB1 transduced cells. CD2-expressing (A) or CD2-RUSH expressing (B) KBM7 cells were transduced with the lentiCRISPRv2-TRIB1 targeting plasmid, Puromycin selected and single cell sorted using FACSAria. DNA was isolated and sequenced. *TRIB1* reference genome, target locus, PAM sequence and the predicted double strand break (DSB) region are indicated. Sequencing results were compared to the reference genome using the SeqMan Pro Software. Genomic alterations in cells were detected and named accordingly. (A) CD2 expressing KBM7 cells: KO 1, 31 bp deletion; KO 2, 5 bp deletion; KO 3, 5 bp deletion; KO 4, 35 bp deletion; KO 5, 16 bp deletion; (B) CD2-RUSH KBM7 cells: KO 1, 5 bp deletion; KO 2, 5 bp deletion; KO 3, 5 bp deletion

Single cell clones of CD2 expressing KBM7 cells and CD2 expressing KBM7 RUSH clones showing deletious mutations were selected and used for further experiments.

2 Protein Secretory Trafficking in *TRIB1* KO cell lines

2.1 FACS analysis of CD2 expressing KBM7 cells

In order to elucidate the effect of *TRIB1* knockout on the secretory pathway, we first performed fluorescence activated cell sorting studies. Similar to the previously conducted genome-wide knockout screening, we observed cell surface expression of CD2 in *TRIB1* knockout cells. Therefore, CD2 expressing KBM7 cells were stained with Phycoerythrin (PE) conjugated anti-CD2 Ab. We used unstained and non-targeted control cells. In non-targeted control cells CD2 expressing KBM7 cells were transduced with the lentiCRISPRv2 vector containing a sgRNA with a random sequence of 20 oligonucleotides. These cells were Puromycin selected, single cell sorted and subjected to a genome check in the same way as the *TRIB1* knockout clones.

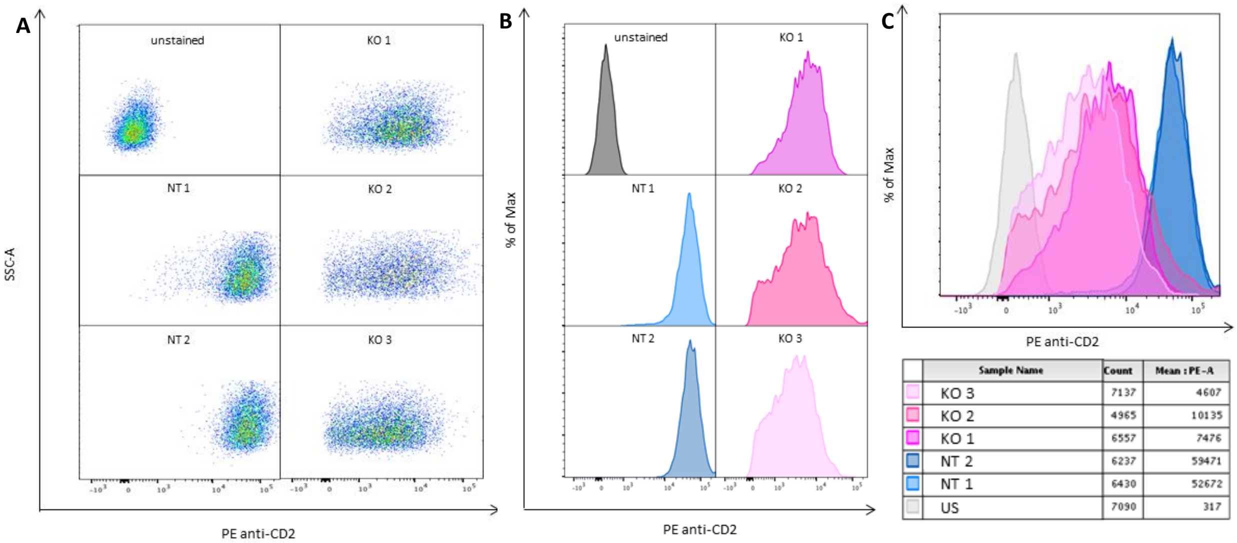

	Sample Name	Count	Mean : PE-A
☐	KO 3	7137	4607
☐	KO 2	4965	10135
☐	KO 1	6557	7476
☐	NT 2	6237	59471
☐	NT 1	6430	52672
☐	US	7090	317

Fig. 11 FACS analysis of CD2 expressing KBM7 cells targeted with gRNA1. Control groups and *TRIB1* knockout cells using gRNA1 were stained with PE conjugated anti-CD2 Ab. (A) Pseudo-color dot plot showing PE fluorescence in relation to sideward scatter. Unstained cells used as negative control group exhibited no PE fluorescence *TRIB1* knockout clones (KO 1, KO 2, KO 3) showed decreased PE fluorescence compared with non-targeted control groups (NT 1, NT 2). (B) Histogram of PE fluorescence. (C) Overlay of histograms shown in (B) Table of cell count and mean fluorescence intensity of PE.

As shown in Figure 11, CD2 cell surface expression of CD2 expressing KBM7 cells was reduced in *TRIB1* knockout cells compared to the nontargeted control groups. While the control group depicts a mean PE fluorescence of about 50 k, *TRIB1* knockout reduces the MPI to about 7 k (KO 1), 10 k (KO 2) and 5 k (KO 3), respectively. In order to ensure that specifically the knockout of *TRIB1* was causing this effect, we targeted *TRIB1* at a second locus (see Fig. 7 and Fig. 10) and checked PE conjugated CD2 cell surface expression via FACS under the same conditions.

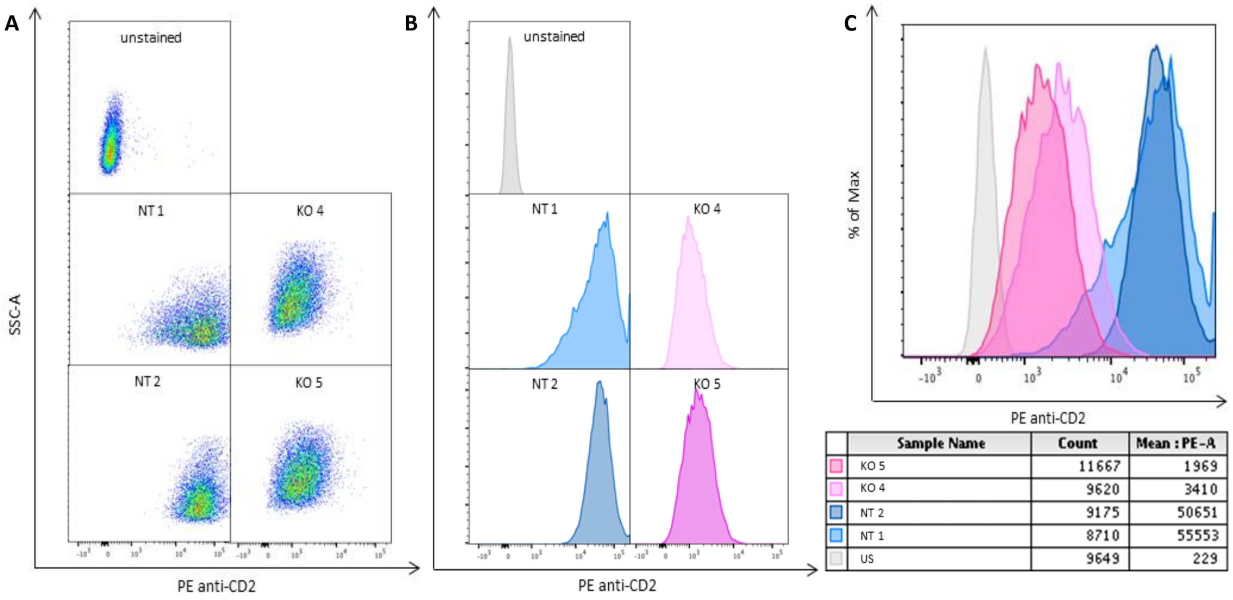

	Sample Name	Count	Mean : PE-A
■	KO 5	11667	1969
■	KO 4	9620	3410
■	NT 2	9175	50651
■	NT 1	8710	55553
■	US	9649	229

Fig. 12 FACS analysis of CD2 expressing KBM7 cells targeted with gRNA2. Control groups and *TRIB1* knockout cells using gRNA2 were stained with PE conjugated anti-CD2 Ab. (A) Pseudo-color dot plot showing PE fluorescence in relation to side scatter. *TRIB1* knockout clones (KO 4, KO 5) showed decreased PE fluorescence compared with nontargeted control groups (NT 1, NT 2). (B) Histogram depicting PE conjugated CD2. (C) Overlay of histograms shown in (B) Table of cell count and mean PE fluorescence.

Again, as indicated in Figure 12, CD2 expression was markedly reduced in *TRIB1* knockout cells targeted with gRNA2 compared to the nontargeted control group. While the control groups show an MPI of about 50 k, PE fluorescence was reduced to 3 k (KO 4) and 2 k (KO 5), respectively.

3 Reconstitution of *TRIB1* KO Cell Lines

In order to verify that the *TRIB1* knockout was crucial for the detected changes in protein trafficking, we reconstituted *TRIB1* in previously knocked out cell lines, hypothesizing that reconstitution should result in a recovery of the phenotype.

3.1 Vector cloning

For *TRIB1* reconstitution, I planned to clone the *TRIB1* complementary DNA sequence (Genescript) into the HA-IRES-RFP-pRRL lentiviral vector. In order to enable sticky end ligation into this vector we produced a MluI-TRIB1-SfaAI amplicon via PCR using Q5 Polymerase and a specific primer set (Tab. 4) inheriting an overhang for recognition sites of restriction enzymes MluI and SfaAI,

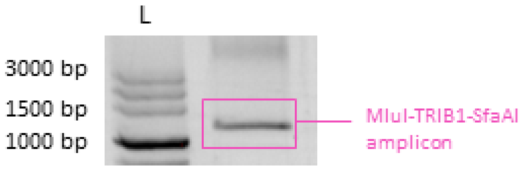
L
3000 bp
1500 bp
1000 bp
MluI-TRIB1-SfaAI amplicon

Fig. 13 MluI-TRIB1-SfaAI amplicon. The MluI-TRIB1-SfaAI amplicon was produced by PCR using Q5 Polymerase and the primers MluI-TRIB1 f and TRIB1-SfaAI r with an indicated length of 1138 bps. The PCR product was subjected to a 1% agarose gel run, visualized using ImageLab, checked the size and extracted from the gel. L, ladder.

Since direct cloning into the lentiviral vector was not successful on several trials, we decided to clone the amplicon into the pMiniT 2.0 cloning vector first in order to add more intermediate steps, that might lead to a clearer view and better management of the source of defect. Therefore, we bluntly ligated the MluI-TRIB1-SfaAI amplicon into the pMiniT 2.0 vector.

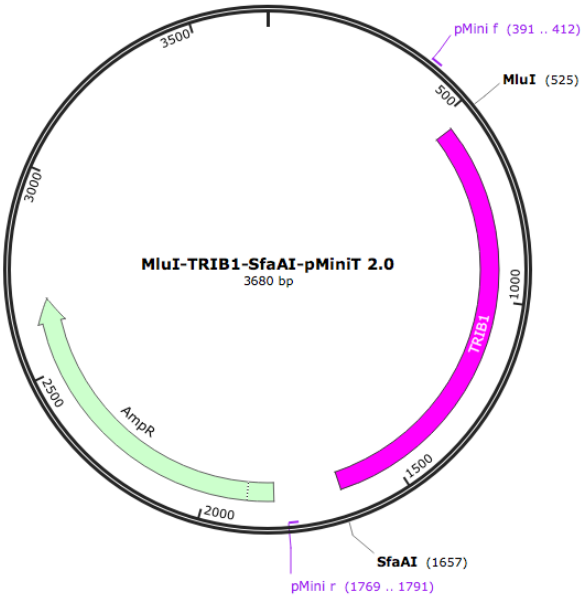
pMini f (391 .. 412)
MluI (525)
500
1000
1500
2000
2500
3000
3500
MluI-TRIB1-SfaAI-pMiniT 2.0
3680 bp
TRIB1
AmpR
SfaAI (1657)
pMini r (1769 .. 1791)

Fig. 14 Constructed MluI-TRIB1-SfaAI-pMiniT2.0 cloning vector for *TRIB1* reconstitution. The MluI-*TRIB1*-SfaAI amplicon was bluntly ligated into the pMiniT2.0 vector. The primers used for the sequencing are shown (pMini f and the pMini r primers).

Successful cloning of the amplicon into the pMiniT 2.0 vector was checked by sequencing using the pMini f and the pMini r primers. After confirming the correct insertion, I cut the MluI-TRIB1-SfaAI-pMiniT2.0 plasmid using the restriction enzymes MluI and SfaAI, subjected the product to a 1% agarose gel run, checked the size of both digestion products (MluI-TRIB1-SfaAI fragment: ~1200 bps, pMini backbone: ~ 2500 bps) and extracted the MluI-TRIB1-SfaAI fragment from the gel.

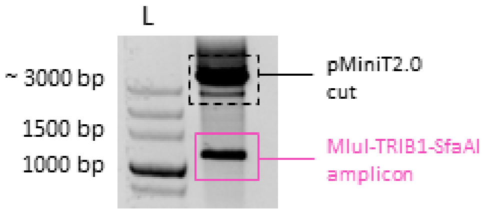
L
~ 3000 bp
1500 bp
1000 bp
pMiniT2.0 cut
MluI-TRIB1-SfaAI amplicon

Fig. 15 Digestion of MluI-TRIB1-SfaAI-pMiniT2.0 cloning vector using MluI and SfaAI. After vector digestion, the digestion product was subjected to an agarose gel run on 1 % agarose, visualized using the ImageLab software and size checked. The MluI-TRIB1-SfaAI fragment was extracted from the gel. L, ladder.

Finally, TRIB1 was cloned into the HA-IRES.RFP-pRRL vector via sticky end ligation. The lentiviral vector was first cut using the restriction enzymes MluI and SfaAI and TRIB1 was inserted into the digested vector.

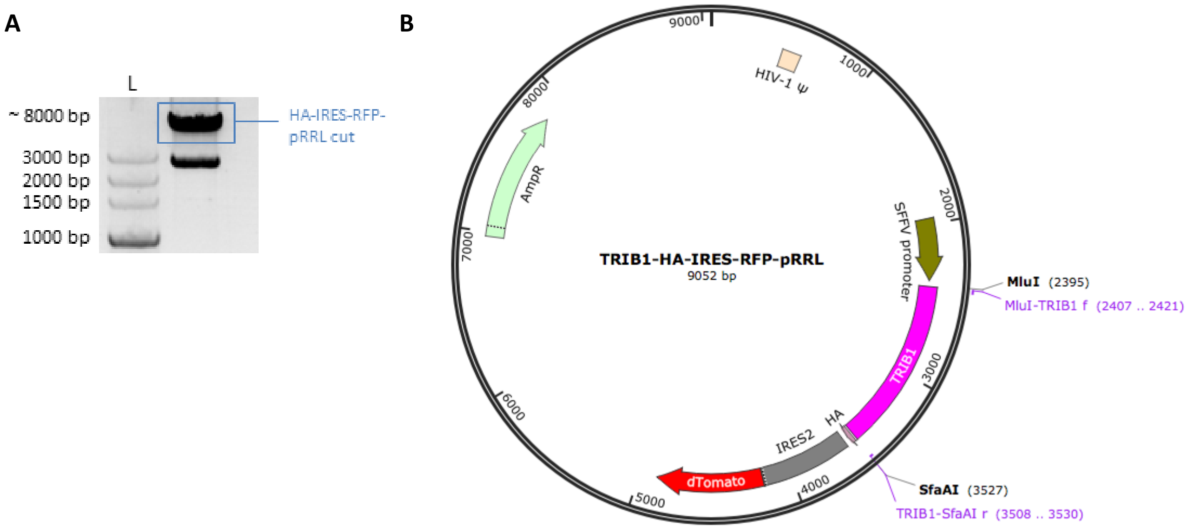
A
B
L
~ 8000 bp
3000 bp
2000 bp
1500 bp
1000 bp
HA-IRES-RFP-pRRL cut
9000
1000
2000
3000
4000
5000
6000
7000
8000
HIV-1 ψ
AmpR
SFFV promoter
TRIB1
HA
IRES2
dTomato
TRIB1-HA-IRES-RFP-pRRL
9052 bp
MluI (2395)
MluI-TRIB1 f (2407 .. 2421)
SfaAI (3527)
TRIB1-SfaAI r (3508 .. 3530)

Fig. 16 TRIB1-HA-IRES-RFP-pRRL vector cloning for *TRIB1* reconstitution. (A) Digestion product of the HA-IRES-RFP-pRRL vector with the restriction enzymes MluI and SfaAI. The upper band corresponding to ~ 8000 bps was extracted from the gel and used for sticky end ligation. (B) Constructed TRIB1-HA-IRES-RFP-pRRL vector for TRIB1 reconstitution. MluI-TRIB1-SfaAI (Fig. 13) was ligated into the HA-IRES-RFP-pRRL vector. The correct insertion was checked by sequencing using the MluI-TRIB1 f and the TRIB1-SfaAI r primers. L, Ladder

The constructed plasmid was checked via sequencing. Subsequently, we transduced this plasmid into the *TRIB1* KO clones (KO 1, KO 2 and KO 3 and RUSH KO 1, KO 2 and KO 3). Upon transduction we sorted the cells showing red fluorescent protein (RFP) expression using FACSAria. Since cells inherited high red fluorescence upon successful transduction of the TRIB1-HA-IRES-RFP-pRRL vector, RFP positive cells were considered to be *TRIB1* reconstituted and named accordingly: KO 1+TRIB1, KO 2+TRIB1, and KO 3+TRIB1 and RUSH KO 1+TRIB1, KO 2+TRIB1 and KO 3+TRIB1.

3.2 Assessment of *TRIB1* targeting and reconstitution

Since TRIB1 was not detectable by immunoblotting in all nontargeted, TRIB1 KO or TRIB1 reconstituted cell lines under various blotting conditions, we investigated TRIB1 mRNA levels by RT-PCR and subsequent gel electrophoresis.

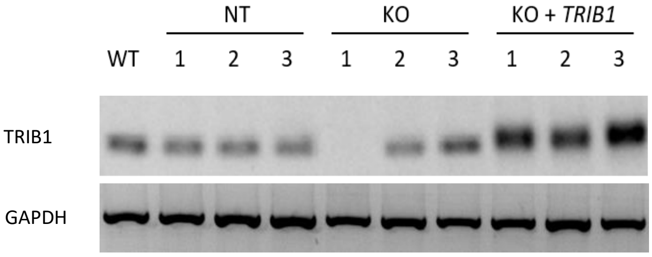

Fig. 17 RT-PCR of TRIB1 cDNA in CD2 KBM7 cell clones. RNA was isolated using the RNeasy Kit and transcribed into cDNA by RT-PCR using the High Capacity cDNA Reverse Transcription Kit. PCR was performed using Onetaq Polymerase and the TRIB1 mRNA f1/r1 primer set (Tab. 8). PCR products were subjected to Agarose electrophoresis. Higher band intensity detected in KO+ *TRIB1* cell clones compared to WT, NT and KO cell clones. cDNA expression varied in KO cell clones depending on cell clone. L, ladder. WT, wildtype. NT, non-targeted. KO, knockout. Bp, bas pairs.

Using three different primer pairs, we detected TRIB1 cDNA levels in CD2 KBM7 WT, nontargeted, *TRIB1* targeted and *TRIB1* reconstituted cell lines. As illustrated for three representative cell clones in Fig. 17, *TRIB1* reconstituted cells overall expressed higher levels of TRIB1 mRNA than KO and nontargeted cells. At the same time we observed altered TRIB1 cDNA levels in TRIB1 targeted cell clones. As depicted in Fig. 11 TRIB1 cDNA expression levels after CRISPR targeting varied depending on the indel mutation. While some cell clones did not express TRIB1 cDNA at all (KO 1), others showed expression levels comparable to nontargeted and wildtype cell lines.

4 Effect of *TRIB1* Reconstitution on Protein Trafficking

4.1 FACS analysis of *TRIB1* KO and *TRIB1* reconstituted CD2 KBM7 cells

In order to observe CD2 cell surface expression in both *TRIB1* KO and *TRIB1* reconstituted cells, we again performed FACS analysis. Therefore, we stained knockout and reconstituted cells with Pacific Blue conjugated anti-CD2 Ab.

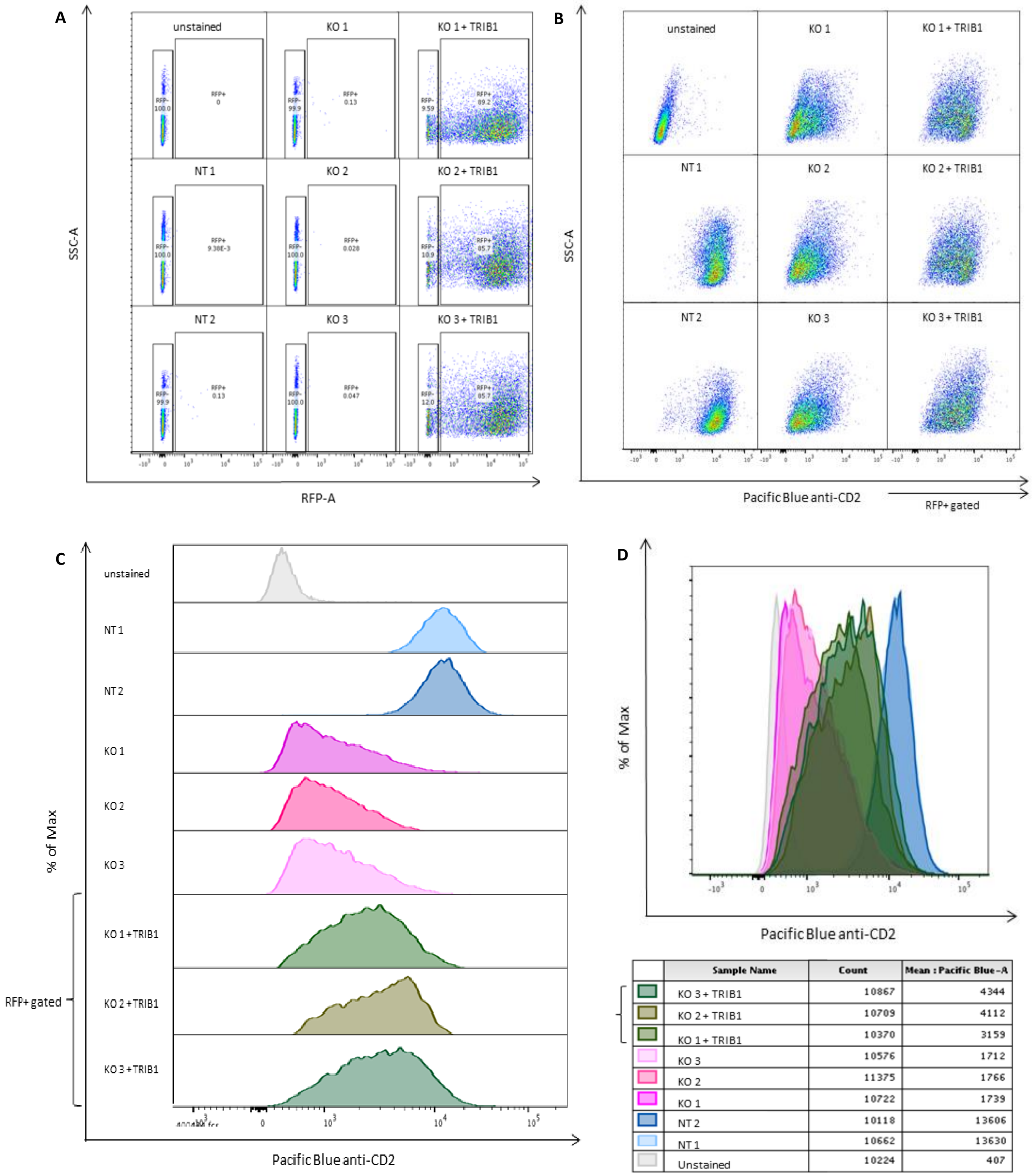

	Sample Name	Count	Mean : Pacific Blue-A
🟩	KO 3 + TRIB1	10867	4344
🟫	KO 2 + TRIB1	10709	4112
🟩	KO 1 + TRIB1	10370	3159
🟪	KO 3	10576	1712
🟥	KO 2	11375	1766
🟪	KO 1	10722	1739
🟦	NT 2	10118	13606
🟦	NT 1	10662	13630
⬜	Unstained	10224	407

Fig. 18 FACS analysis of CD2 expressing KBM7 cells upon *TRIB1* reconstitution. *TRIB1* knockout cells were transduced with the TRIB1-HA-IRES-RFP-pRRL vector and RFP-positive cells were sorted. For FACS analysis, cells were stained with Pacific Blue conjugated anti-CD2 Ab. (A) Pseudo-color dot plot diagram of RFP expression. Unstained control (US), nontargeted control groups (NT 1, NT 2) and knockout cells (KO 1, KO 2, KO 3) were RFP negative, whereas transduced cells (KO 1+TRIB1, KO 2 +TRIB1, KO 3 +TRIB1) were largely RFP positive. (B) Pseudo-color dot plot of Pacific Blue fluorescence. RFP positive population was gated in *TRIB1* reconstituted cells. (C) Histogram of Pacific Blue fluorescence. (D) Upper panel, overlay of histograms shown in (C), indicating that CD2 expression has partly recovered upon *TRIB1* reconstitution. Lower panel, table with cell count and Mean fluorescence intensity of Pacific Blue.

As shown in Figure 18 A, reconstitution of *TRIB1*- RFP led to a high percentage of RFP positivity among TRIB1-HA-IRES-RFP-pRRL transduced cells (KO 1+ TRIB1, KO 2+TRIB1, KO 3+TRIB1) while control groups (US, NT 1, NT 2) and *TRIB1* knockout cells (KO 1, KO 2, KO 3) were overall RFP negative.

When observing the CD2 cell surface expression of each cell clone in the pseudo-color dot plot (Fig. 18 B) and the histogram (Fig.18 C), *TRIB1* knockout and reconstituted cells both showed a decrease in Pacific Blue fluorescence compared to the nontargeted control groups. However, as depicted in the histogram overlays (Fig. 18 D), *TRIB1* reconstituted cells showed a partial recovery in CD2 cell surface expression compared to the *TRIB1* knockout cells. The recovery was also affirmed by the Mean Pacific Blue Fluorescence in each cell group. While the MPI of the nontargeted control group ranged at 13 k, knockout cells had an average MPI of 1 k whereas reconstituted cells showed an MPI of 3 k- 4 k.

4.2 Imaging of CD2-RUSH KBM7 cells

Next, we used the RUSH system to investigate intracellular CD2 trafficking (see IV, 8.1 for the RUSH method). Therefore, we added Biotin at several timepoints, fixed and permeabilized the cells and stained several cell compartments in the protein secretion pathway. Subsequently we observed the localization of GFP tagged CD2 within the cell via confocal microscope upon biotin treatment triggering the release of CD2-GFP from the ER.

A RUSH NT 1

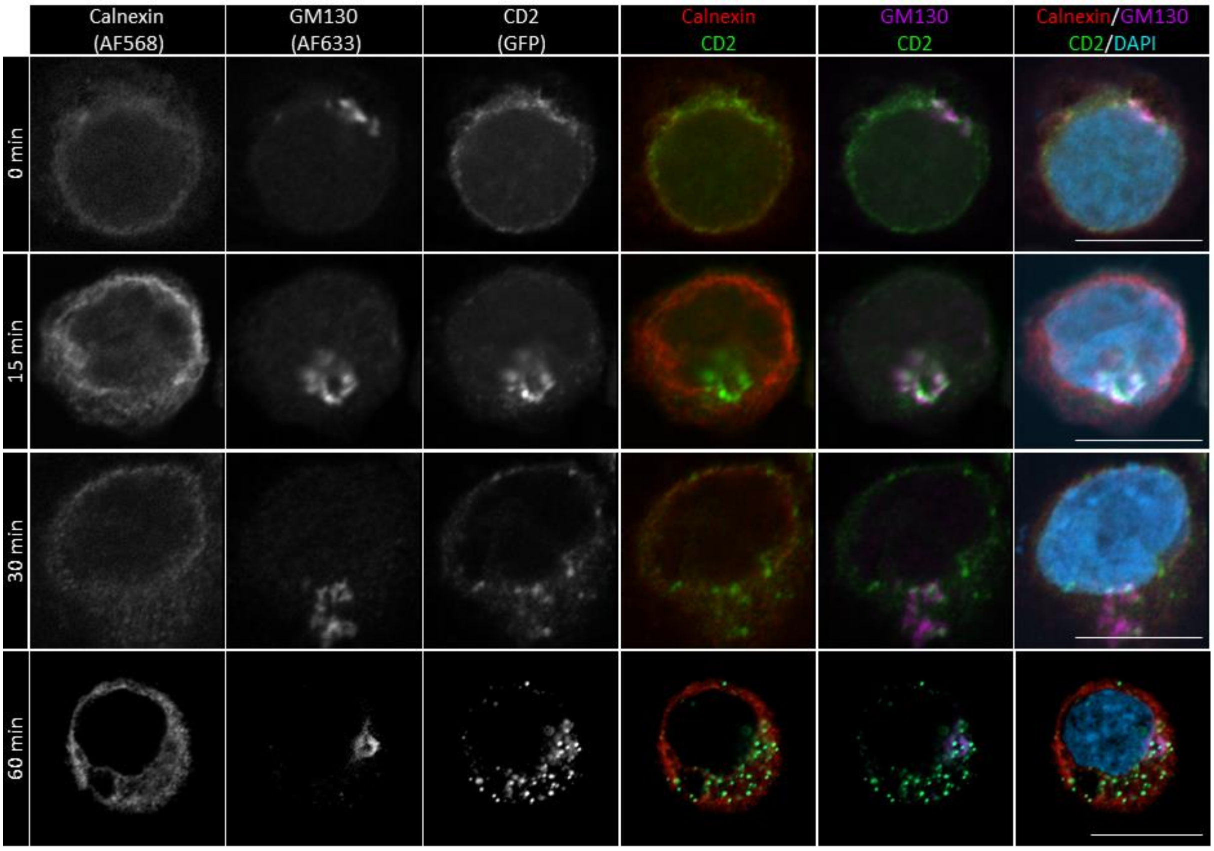
Calnexin
(AF568)
GM130
(AF633)
CD2
(GFP)
Calnexin
CD2
GM130
CD2
Calnexin/GM130
CD2/DAPI
0 min
15 min
30 min
60 min

B RUSH KO 1

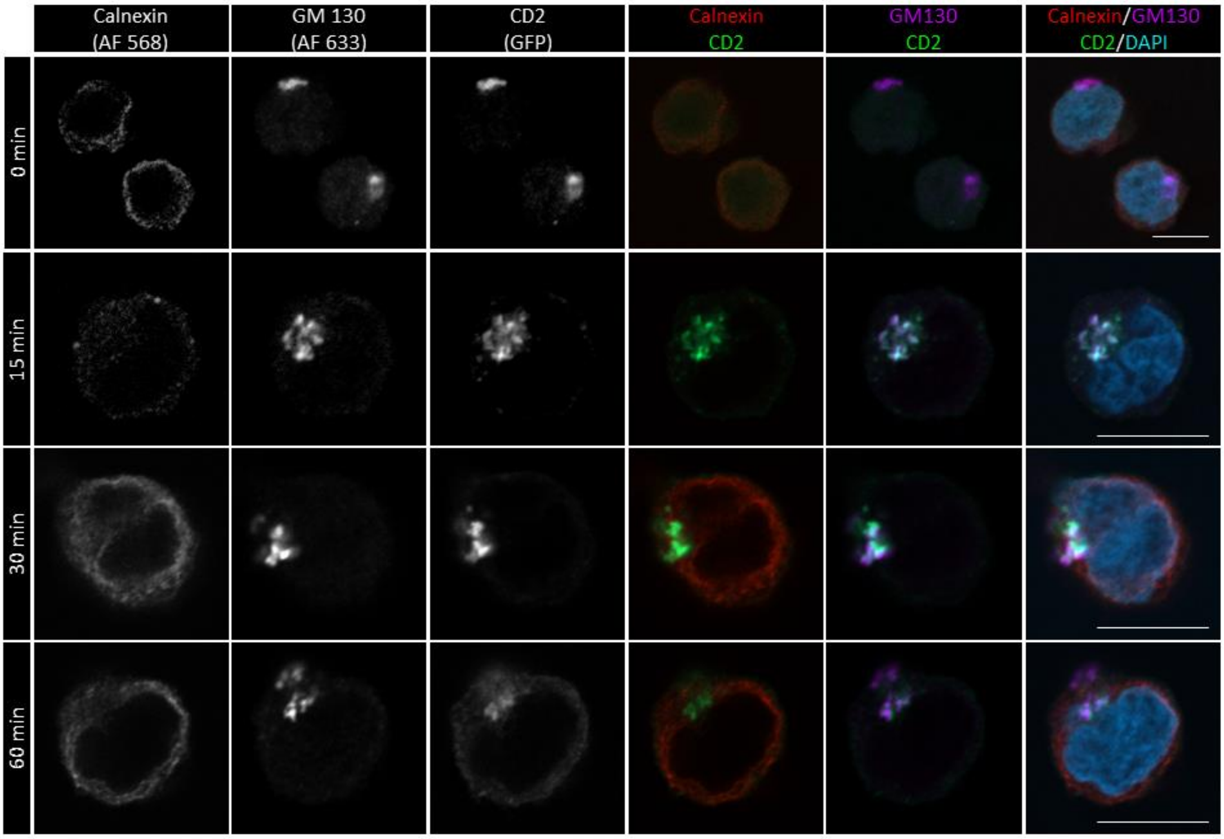
Calnexin
(AF 568)
GM 130
(AF 633)
CD2
(GFP)
Calnexin
CD2
GM130
CD2
Calnexin/GM130
CD2/DAPI
0 min
15 min
30 min
60 min

RUSH KO 2

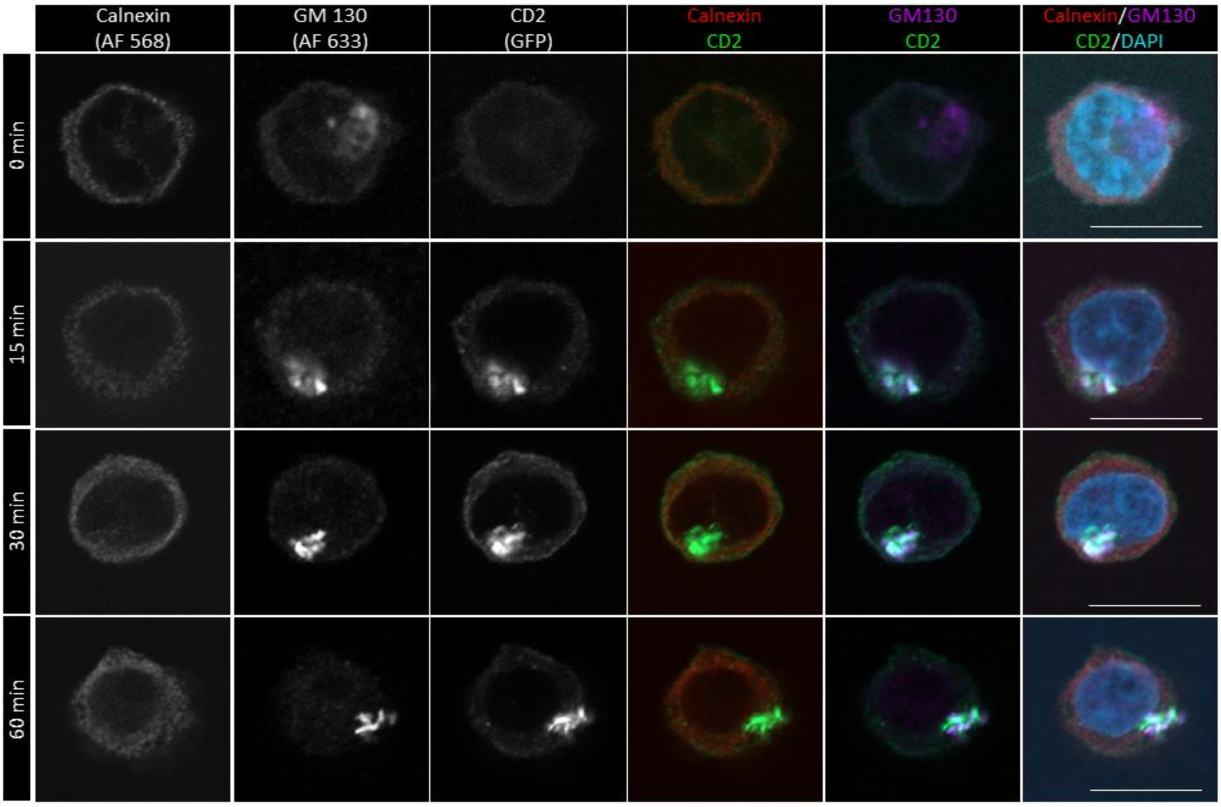
Calnexin (AF 568)
GM 130 (AF 633)
CD2 (GFP)
Calnexin CD2
GM130 CD2
Calnexin/GM130 CD2/DAPI
0 min
15 min
30 min
60 min

RUSH KO 3

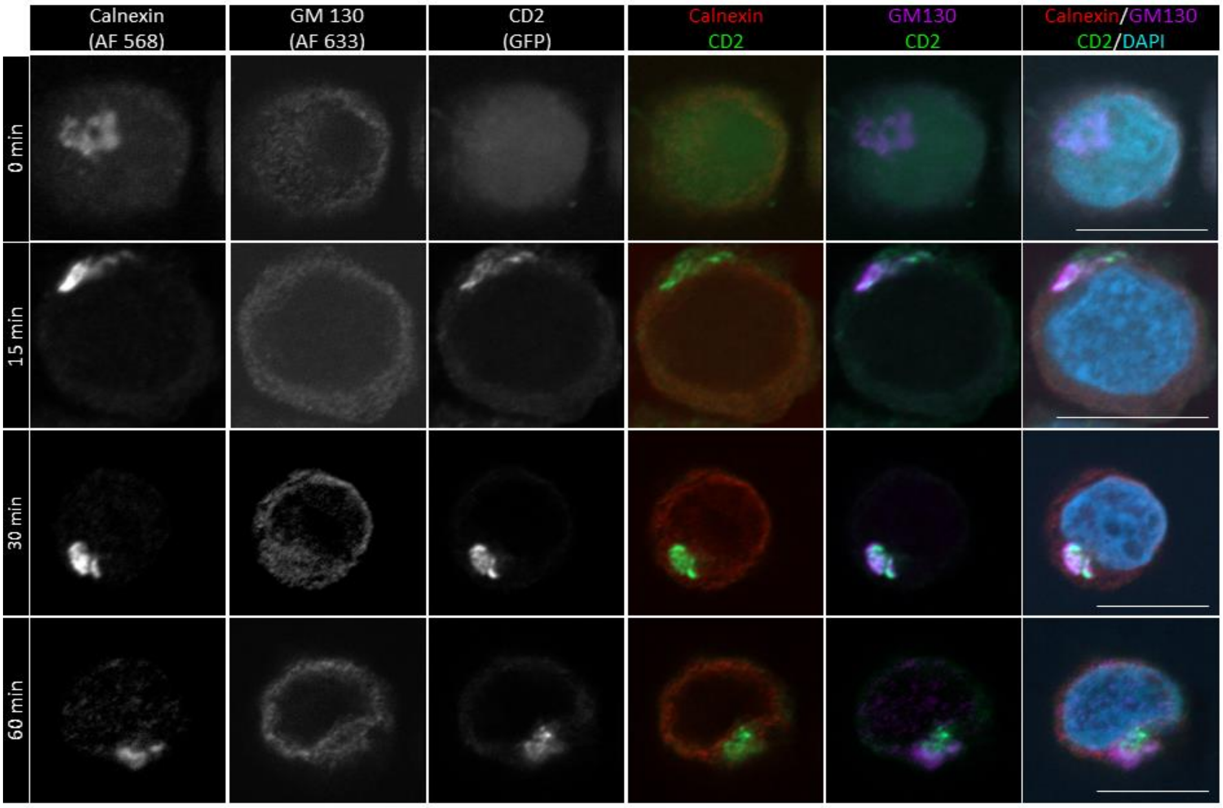
Calnexin (AF 568)
GM 130 (AF 633)
CD2 (GFP)
Calnexin CD2
GM130 CD2
Calnexin/GM130 CD2/DAPI
0 min
15 min
30 min
60 min

c

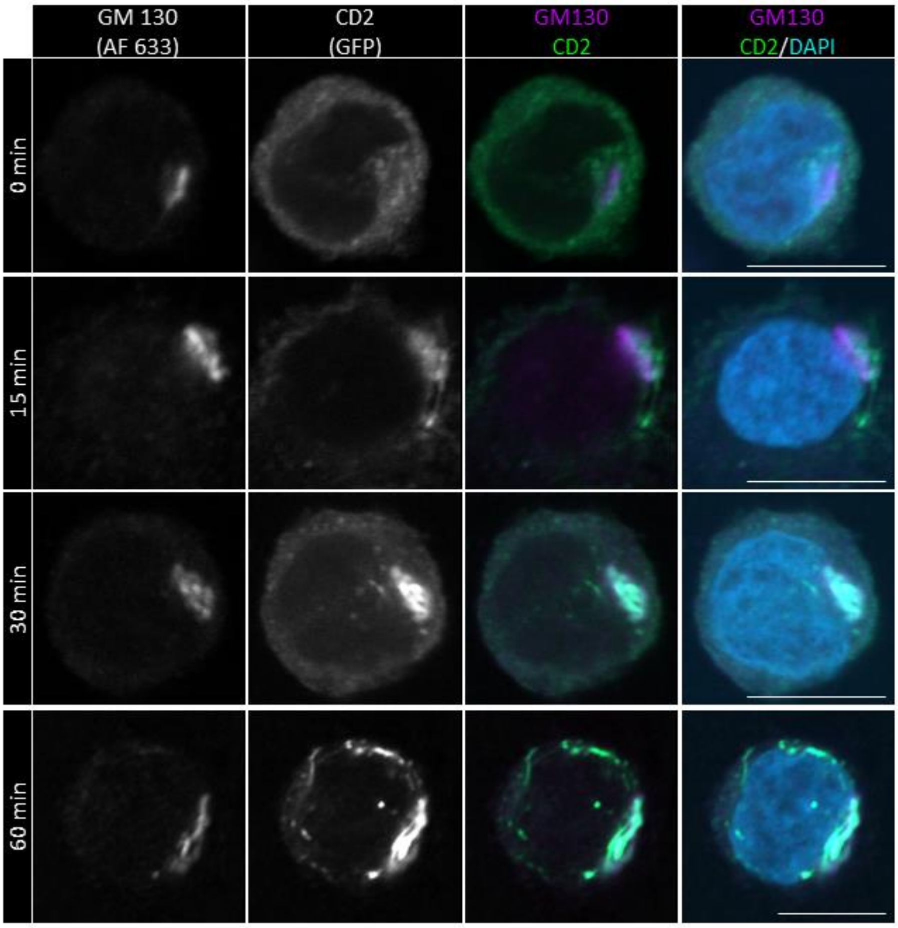
GM 130 (AF 633)
CD2 (GFP)
GM130 CD2
GM130 CD2/DAPI
0 min
15 min
30 min
60 min

RUSH KO 1 + *TRIB1*

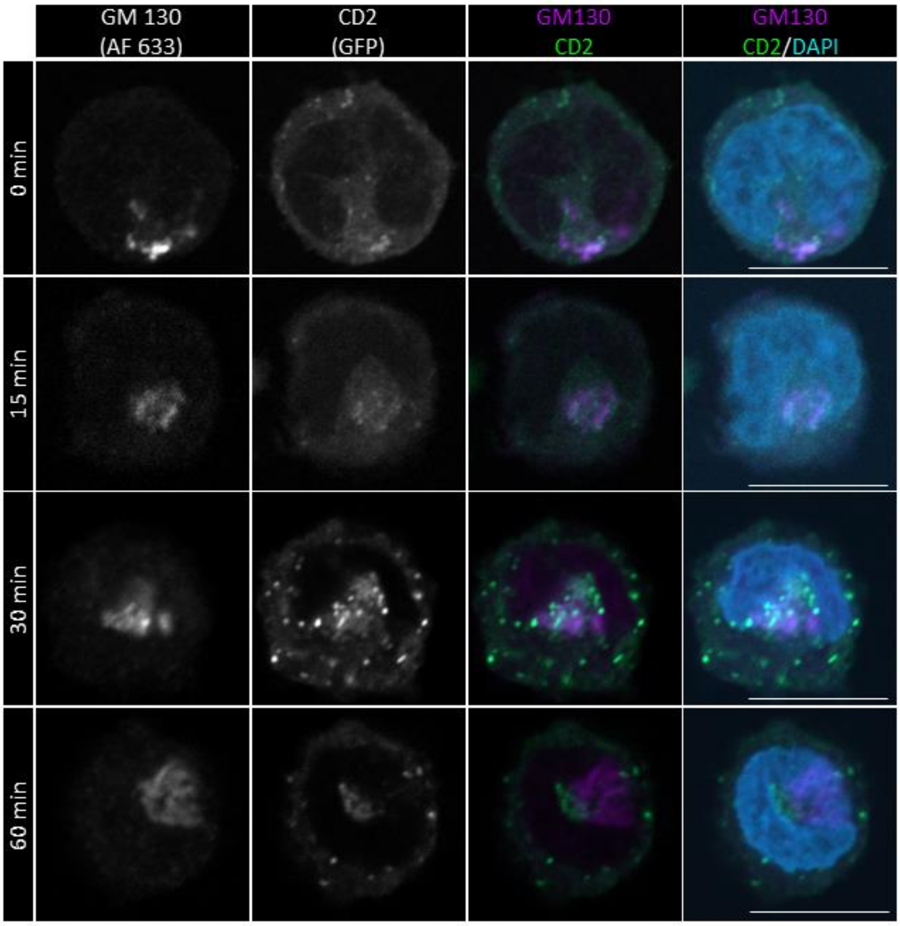
GM 130 (AF 633)
CD2 (GFP)
GM130 CD2
GM130 CD2/DAPI
0 min
15 min
30 min
60 min

RUSH KO 2 + *TRIB1*

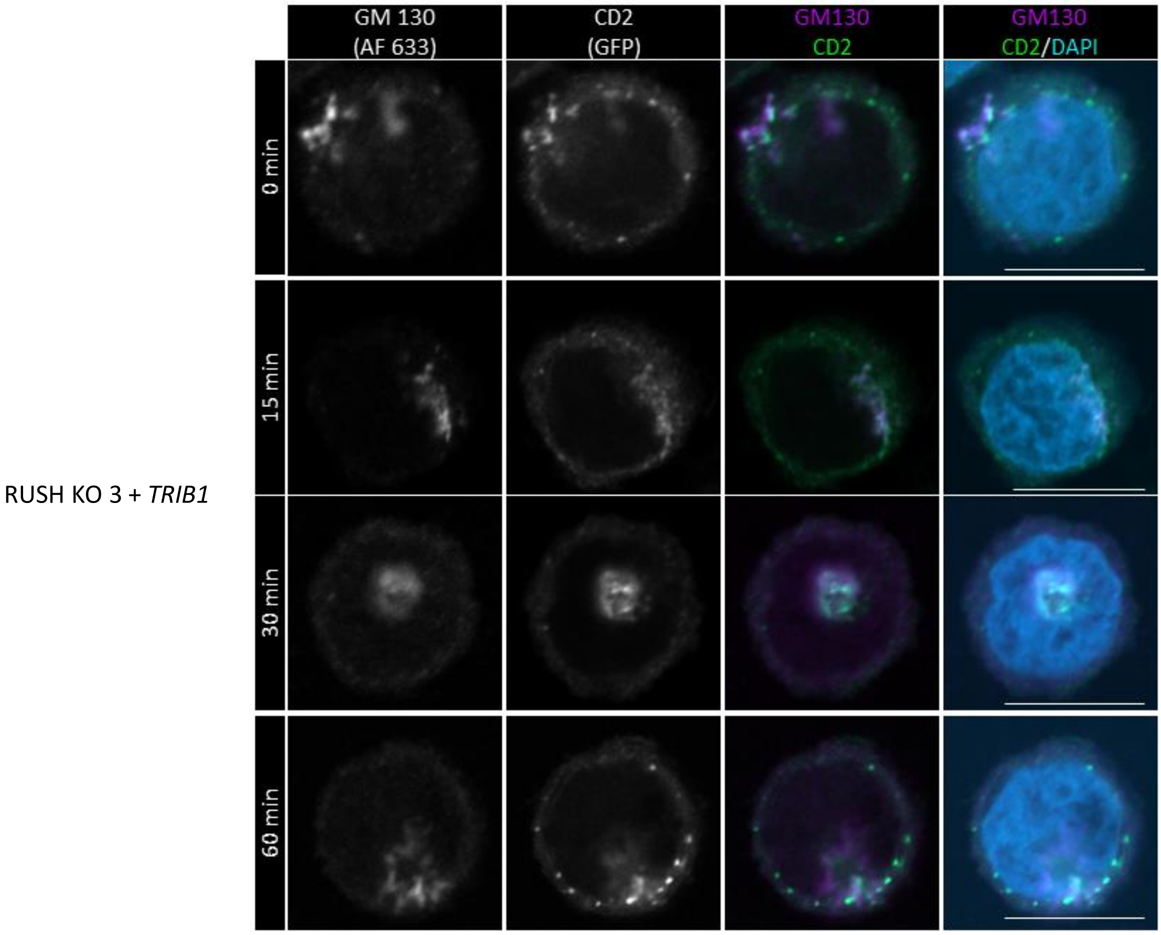

Fig. 19 Confocal imaging of CD2-RUSH-KBM7 cells. Cells were subjected to biotin treatment for indicated time duration, fixed and permeabilized. The Golgi complex was stained with mouse anti-GM130 primary Ab and anti-mouse AF633 secondary Ab. The endoplasmic reticulum was stained with rabbit anti-Calnexin primary Ab and anti-rabbit AF568. For *TRIB1* reconstituted cells (KO 1 + *TRIB1*, KO 2 + *TRIB1*, KO 3 + *TRIB1*), cells were stained with anti-GM130 Ab. The cell nucleus was stained using DAPI. Blue, DAPI; Green, GFP-tagged CD2; Red, Calnexin; Violet, GM130. (A) CD2-RUSH-KBM7 nontargeted control cell. At 0 min of Biotin treatment GFP-CD2 colocalized with Calnexin upon 15 min of treatment, GFP-CD2 colocalized with GM130. After 30 min of Biotin treatment GFP-CD2 is diffusely spread and remains diffusely localized after 60 min. (B) CD2-RUSH-KBM7 *TRIB1* knockout cell lines (KO 1, KO 2, KO 3). GFP-CD2 was localized in the ER at timepoint 0 min and colocalized with GM130 after 15 min, 30 min and 60 min of Biotin treatment. (C) CD2-RUSH-KBM7 *TRIB1* reconstituted cells (KO 1+ *TRIB1*, KO 2+ *TRIB1*, KO 3+ *TRIB1*). At 0 min of Biotin treatment GFP-CD2 was located inside the cell, surrounding the nucleus, upon 15 min, it colocalized with GM130 and starts diffusely spreading out at 30 min upon Biotin addition. Scale bar: 10µm

In the nontargeted control group (Fig. 19 A), GFP tagged CD2 was initially localized to the ER at 0 min, then trafficked to the Golgi apparatus after 15 min, and lastly was detectable in after 30 min and 60 min, respectively. In contrast, in *TRIB1* KO clones (Fig. 19 B), GFP-CD2 was localized to the ER at 0 min, trafficked to the Golgi apparatus after 15 min and remained at the Golgi after 30 min and 60 min. In TRIB1 reconstituted cells (Fig. 19 C) GFP-CD2 was localized intracellularly surrounding the nucleus at 0 min, localized to the Golgi apparatus at 15 min and partly at 30 min of Biotin treatment and then spread out to vesicles similar to wildtype control cells. Thus, in the absence of TRIB1, trafficking of CD2 was perturbed.

5 ER Stress Response to Tunicamycin Treatment

In order to investigate, whether *TRIB1* knockout might have an effect on ER homeostasis and therefore perturb CD2 trafficking, we checked the response of *TRIB1* KO cells to Tunicamycin treatment. It is widely appreciated that Tunicamycin can be used to activate the unfolded protein response (UPR) via its master regulators IRE1a and PERK. While IRE1a is responsible for XBP1 mRNA splicing, which upregulates UPR target genes, CHOP, a more downstream protein of PERK plays an important role for ER stress-mediated apoptosis. Therefore, we treated CD2 expressing KBM7 cells with Tunicamycin for the indicated time, extracted RNA and reverse transcribed it to cDNA using the High Capacity cDNA Reverse Transcription Kit. Subsequently we performed a PCR using the Onetaq polymerase and XBP1 and CHOP specific primer sets and investigated PCR products by electrophoresis on 1.5% Agarose gel. GAPDH was used loading control.

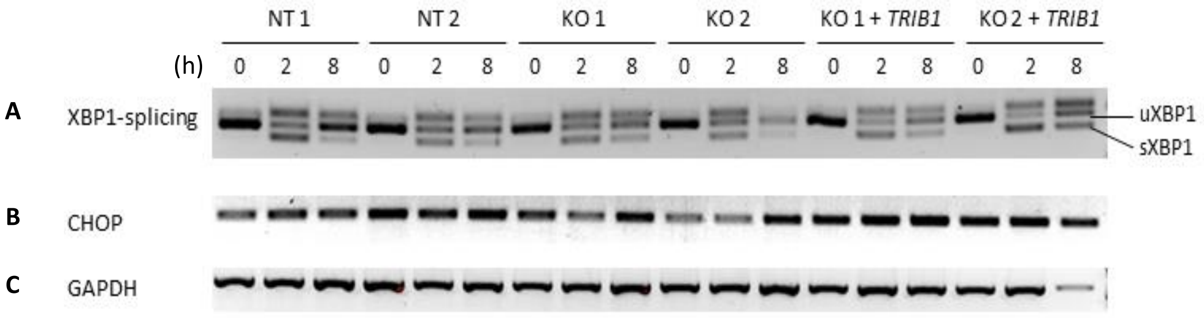

Fig. 20 RT-PCR of UPR genes after Tunicamycin treatment. Cells were subjected to Tunicamycin treatment for indicated time duration, RNA was isolated using the RNeasy Kit and transcribed into cDNA by RT-PCR using the High-Capacity cDNA Reverse Transcription Kit. PCR was performed using Onetaq Polymerase and PCR products were subjected to Agarose electrophoresis (A) XBP1 signal divided in un-spliced (uXBP1) and spliced (sXBP1). No significant difference in band intensity between NT, KO and KO+TRIB1 cells indicating similar activation of UPR via the IRE1a pathway after Tunicamycin treatment. (B) CHOP signal, no difference in band intensity between NT, KO and KO+TRIB1 cells indicating no significant difference in PERK activation after 2h or 8h of Tunicamycin treatment. (C) GAPDHl as loading control. h, hours

Figure 19 indicates UPR activation in TRIB1 KO cells compared to nontarget and reconstituted cells. The mRNA ratio of spliced XBP1 to un-spliced XBP1 was not significantly different between nontargeted, TRIB1 KO and TRIB1 reconstituted cells at both timepoints. At the same time, CHOP mRNA levels were similar in nontargeted, TRIB1 KO and TRIB1 reconstituted cells. This finding suggests that TRIB1 alteration does not affect Tunicamycin induced UPR activation.

VI Discussion

Due to the complexity and vast variety of proteins transiting the secretory pathway, it is not surprising that perturbations are associated with numerous human diseases. For example, protein misfolding leads to diseases such as phenylketonuria, cystic fibrosis, familial neuro hypophyseal diabetes insipidus and Parkinson's disease (Gregersen et al., 2006). Previous findings suggest that chronic ER stress contributes to the degeneration of dopaminergic neurons of the substantia nigra (Silva et al., 2005). Apart from protein folding, many other parts of the secretory pathway can be disturbed, causing severe congenital diseases (Amara et al., 1992).

The role of the secretory pathway in neutrophil disorders remains poorly investigated. To get an unbiased overview of genes involved in this pathway in myeloid cells, we performed a CRISPR based large-scale genome wide screen. In this screen, CD2-expressing KBM7 cells, a near haploid chronic myelogenous leukemia (CML) cell line, were utilized to monitor the secretory pathway. Since the trafficking of CD2 reporter molecule is affected by damage of the secretory pathway, knockout of genes with function in the pathway downregulates the cell surface expression level of CD2. In this screen, 325 genes were discovered as potential players in the secretory pathway in myeloid cells. However, further individual validations are required to confirm the function of each candidate gene, since the disruption of the secretory pathway is not the only reason to affect the reporter expression. Also, the possibility of false-positive hits in this kind of large-scale screening needs to be excluded.

This thesis addresses the topic to functionally validate the role of *TRIB1*, one of the significant genes found in the screen, as promising novel candidate in controlling the secretory pathway.

1 TRIB1 as Orchestrator of the Secretory Pathway

In line with our prior screen, *TRIB1*-targeted gene disruption by CRISPR/Cas9 resulted in lower CD2 expression compared to nontargeted sgRNA transduced control cells, indicating an error within the secretory pathway. This was further confirmed by individual *TRIB1* knockout clones of KBM7 cells (Fig. 11, Fig. 12). Furthermore, this phenotype was restored by *TRIB1* reconstitution, suggesting a correlation between the presence of TRIB1 and proper protein trafficking, excluding the possibility of off-target effect in CRISPR/Cas9-mediated genome editing (Fig. 18). This result suggests a novel function of TRIB1 controlling the protein secretory pathway in myeloid cells.

In order to investigate the detailed role of TRIB1 in the secretory pathway, we further assessed at which step protein secretion was perturbed by TRIB1 deficiency. For this, we implemented the RUSH system (Boncompain et al., 2012). Using this method, we were able to track intracellular, time dependent CD2 reporter protein trafficking by fluorescence microscopy. We observed that *TRIB1* knockout cells showed protein accumulation in the Golgi apparatus, whereas CD2 was spread out toward the plasma membrane in control cells after 60 min of Biotin treatment (Fig. 19). Again, this phenotype was restored by *TRIB1* reconstitution (Fig. 19). Our results therefore suggest that TRIB1 is an orchestrator of the secretory pathway most presumably within the Golgi compartment.

2 Determining TRIB1's Roles

TRIB1 is a member of the Tribbles (TRIB) homolog pseudo-kinases family, which is a subfamily of Ca^{2+}/Calmodulin activated protein kinase but lack the catalytic activity. Despite the lack of catalytic activity, TRIB1 is known to play roles in multiple cellular biology, such as cell differentiation, proliferation, and metabolism, working as an adapter or scaffolding protein. The C-terminus region of TRIB1 is responsible for protein interaction with transcription factors, proteasome subunits or signal transduction molecules in a cell specific manner. For example, TRIB1 binds COP1, an E3 ubiquitin ligase, to facilitate the ubiquitin ligase complex, which leads to target protein degradation.

TRIB1 has also been related to human diseases before. Especially, TRIB1's role in immune mediated diseases has been extensively studied. Increased TRIB1 expression has been linked to myeloid cell neoplasms such as AML (Yokoyama et al., 2012; Yoshino et al., 2021) and Multiple Myeloma (Chen et al., 2020). It is also emphasized that TRIB1 expression correlates with solid tumor development including Hepatocellular Carcinoma (Ye et al., 2017) and Prostate Cancer (Shahrouzi et al., 2020). Additionally TRIB1 has been associated with diverse autoimmune disorders such as Systemic Lupus Erythematosus (Simoni et al., 2018) and Inflammatory Bowel Disease (Jostins et al., 2012). Interestingly TRIB1 expression levels vary among different immune cell subsets. While it is highly expressed in monocytes and Tregs, CD8+ T cells and NK cells show low expression levels (Danger et al., 2022).

Several groups have reported, that TRIB1 plays a critical role in myeloid cell differentiation. For instance, Trib1 deficient mice show a severe decrease of M2-like macrophages indicating its important role in macrophage lineage differentiation (Satoh et al., 2013). Additional studies suggest that TRIB1 regulates the M1/M2 macrophage polarization via the JAK/STAT signaling pathway (Arndt et al., 2018; McMillan et al., 2021). Moreover, Trib1 knockout mice showed a lack of eosinophils and increased neutrophils, suggesting Trib1's important role for early granulocyte lineage differentiation (Mack et al., 2019). The detailed mechanism in the regulation of myeloid cell differentiation by TRIB1 remains to be elucidated. Since the proper protein secretory process is sufficient for cell homeostasis, disruption of the secretory pathway can influence the cell differentiation efficiency and orientation. It is important to clarify the molecular basis of the protein secretory pathway in respective cell types to understand not only cellular proteostasis but also the comprehensive cell developmental system.

In prostate cancer cells, TRIB1 regulates expression of GPR78 and several other ER chaperons supporting cell survival and growth (Mashima et al., 2014). Since ER chaperon activity is critical in the secretory pathway, we investigated the impact of TRIB1 absence on ER homeostasis and function in KBM7 cells. For this purpose, we evaluated ER stress response after Tunicamycin, an ER stressor, treatment. However, subsequent detection of the UPR mediators XBP1 and CHOP showed no significant changes in mRNA levels, suggesting that these ER homeostasis mediating pathways were not affected by TRIB1 alteration in myeloid cells.

Collectively, our studies revealed that *TRIB1* deletion resulted in protein accumulation within the Golgi apparatus not affecting ER homeostasis. While Golgi homeostasis seemed impaired by *TRIB1* knockout, reconstitution of TRIB1 restored Golgi secretory function. Considering the cytosolic and nuclear localization of TRIB1, indirect role on the regulation of Golgi homeostasis is presumed. For instance, TRIB1 might control the protein degradation of negative regulators in the secretory pathway at Golgi. It is also interesting, that TRIB1 has been linked to the MEK1/ERK pathway. In acute myeloid leukemia (AML), TRIB1 overexpression has been associated with increased MEK1/ERK activity due to enhanced ERK phosphorylation (Jin et al., 2007). This leads to inhibition of apoptosis and increased myeloid cell proliferation resulting in leukemia (Yokoyama et al., 2010). In colorectal cancer, TRIB1 was found to promote cell migration by activating the ERK pathways (Y. Wang et al., 2017). During mitosis in mammalian cells, Golgi-based checkpoint needs to be satisfied to enable cell cycle progression (Rabouille & Kondylis, 2007; Sütterlin et al., 2002). When Golgi integrity is ensured, Golgi fragmentation is initiated via the MEK1 pathway (Acharya et al., 1998). Moreover, ERK1 phosphorylates GRASP65, which regulates Golgi structure remodeling in interphase (Bisel et al., 2008). Thus, MEK1/ERK activity, which is enhanced by TRIB1-ERK1 interaction, is involved in diverse cellular activities including organization of the Golgi. Therefore, we propose that TRIB1 not only orchestrates secretory trafficking, but beyond that possibly regulates cell reproduction and differentiation via the Golgi apparatus likely via the MEK1/ERK pathway.

3 Challenges and Limitations of this Project

We targeted *TRIB1* following the well-established CRISPR/Cas9 cloning protocol (Ran et al., 2013). According to previous data, the active domain of TRIB1 is at the protein’s C-Terminus (Jamieson et al., 2019). Using the program UniprotKB we were able to identify the exact locus of COP1 and MAPK binding within the protein. Since these two binding areas are crucial for TRIB1 interaction we targeted that location (Kung & Jura, 2019; Yokoyama et al., 2010). Following the CRISPR/Cas9 protocol, we were quickly able to generate *TRIB1* knockout cell lines.

For *TRIB1* reconstitution, we cloned the TRIB1 cDNA sequence into the HA-IRES-RFP-pRRL vector and transduced it into *TRIB1* KO cell lines by lentiviral transfection. We first tried direct cloning into the lentiviral vector which was unsuccessful. Therefore, we utilized a cloning vector as intermediate step. In contrast to an expression vector such as pRRL, cloning vectors only enable DNA storing and gene propagating in bacteria, but not transcription and translation of the gene into a functional protein product (Carter & Shieh, 2015). By increasing the number of steps during vector cloning we tried to ensure better troubleshooting and quality control. We selected successfully transfected cells by RFP fluorescence. Overall reconstituting *TRIB1* knockout cell lines was challenging.

Off-target binding caused by similarities of genomic loci is not uncommon among sgRNA mediated Cas9 activation. In order to address this issue, we used two different sgRNAs (Duan et al., 2014; Zhang et al., 2015). We then amplified the genomic target segment of each cell clone, sequenced these DNA amplicons, and detected indel mutations using the Software SeqManPro. Cas9 cleavage was observed in most of the single cell clones.

Since only the proposed target area was investigated, the issue of Cas9 off-target binding cannot be fully excluded. In general, the targeting specificity of Cas9 is regulated by the 20 nt sgRNA sequence and the adjacent PAM motif. Commonly Cas9 cleaves about 3bp upstream of the PAM. However off-target mutagenesis remains a major concern (Fu et al., 2013; Hsu et al., 2013; Pattanayak et al., 2013). At the same time, recent studies revealed that even though mismatches are allowed in the PAM-distal part of the sgRNA sequence, only a few off-target sites were substantially modified *in vivo* (Kuscu et al., 2014). The most comprehensive insight into CRISPR targeting specificity and off-target mutagenesis would probably be shed by a whole genome sequencing of each targeted cell clone. However, this approach would require extensive sequencing resources as well as special readout strategies going past the objective and frame of this project. Even though any indel alteration can cause abnormal mRNA transcription or protein translation, frameshift inducing mutations are most likely to cause a premature termination codon (PTC) leading to nonsense-mediated decay resulting in complete protein deletion (Garneau et al., 2007). Therefore, we selected cell clones that showed deletions not divisible by three in our Sanger sequencing results. Additionally, we picked knockout clones differing in size and location of indel mutation. This way a higher diversity of *TRIB1* editing was achieved. However, a complete protein knockout is not guaranteed by this method.

To evaluate TRIB1 protein deletion, we aimed to assess protein expression levels by Immunoblotting. However, using the commercial Antibody (Abcam) we were unable to detect TRIB1 under various experimental conditions in nontargeted, *TRIB1* knockout and *TRIB1* reconstituted cell lines. It has been stated in literature, that TRIB1 is commonly undetectable due to its instability and fast degradation after protein translation (Soubeyrand et al., 2016). This could be an explanation for our immunoblotting results. Treatment with proteasome inhibitor like MG132 might solve this issue enabling TRIB1 to escape from rapid protein degradation.

We therefore investigated TRIB1 mRNA levels by RT-PCR and subsequent gel electrophoresis. Overall *TRIB1* reconstituted cells showed higher levels of TRIB1 mRNA than both knockout and nontargeted cells, indicating the successful transduction. Using three different primer pairs, we observed reduced, but still detectable TRIB1 cDNA in some knockout cell lines indicating mRNA presence even after CRISPR induced frameshift mutagenesis. This seems to be a common issue in CRISPR-based genome editing, since about 50% of CRISPR targeted cell panels with presumed gene knockouts show detection of aberrant mRNA or protein products (Tuladhar et al., 2019). These foreign protein products emerge because distinct inserted mutations promote conversion of pseudo-mRNAs with a PTC into protein encoding molecules (Tuladhar et al., 2019). In line with this publication, the detected mRNA in *TRIB1* knockout cells was deviant in size. Another explanation for residual mRNA after *TRIB1* frameshift mutation could be, that only small genomic regions close to the C-terminus were modified, making it likely for N-terminal sequences to still be transcribed. It is widely appreciated that foreign mRNA is degraded rapidly via the nonsense-mediated mRNA decay pathway (Baker & Parker, 2004). Both decreased mRNA levels and dysmorphology after CRISPR targeting led us to the presumption, that protein translation was impaired. For future studies it is demanded to confirm TRIB1 protein deletion in our knockout cell lines. Nonetheless, recovery of phenotype in *TRIB1* frameshifted clones by reconstitution strongly suggests successful disruption of TRIB1 gene without unintended targeting to other coding genes.

In this study, CD2 was utilized as a reporter protein to evaluate the protein trafficking. CD2 is known to be expressed on the cell surface after passing through the protein secretory pathway from the ER to the plasma membrane. However, CD2 is not endogenously expressed in KBM7 cells. Although it is selected as typical transmembrane protein, dysregulation of CD2 trafficking does not invariably imply the disturbance of protein trafficking in general. Further validation using various endogenous membrane proteins and secretion proteins is required to finally conclude the sufficiency of TRIB1 in the secretory pathway.

From microscopy observation, TRIB1 is supposed to play a role at Golgi apparatus, not in the ER. In the future the molecular basis of TRIB1-mediated control of Golgi homeostasis needs to be clarified to understand this novel function of TRIB1. Since cell-specific function of TRIB1 depends on its binding partners, it is crucial to define which protein interaction regulates the secretory pathway. Addressing if TRIB1-MEK1 interaction is sufficient for Golgi homeostasis should have the highest priority. On the other hand, in the case that COP1 binding is important, the next question will be which ubiquitination target molecules are mediated by the TRIB1-COP1 axis. It is possible that unknown interactors of TRIB1 in myeloid cells have a pivotal role in the secretory pathway. Recently reported interactome data will exploit further analysis (Hernández-Quiles et al., 2021). To grasp the impact of TRIB1-mediated regulation of the secretory pathway, not only protein trafficking but also a variety of cellular biology such as cell proliferation, differentiation and apoptosis need to be explored using various cells including primary cells or iPSC-derived cells. Detection systems of the secretory pathway employed in this study are simple and easy to apply to these other cell types. Whether TRIB1's role in protein trafficking is cell type-specific or not is another concern. Since TRIB1 is reported to associate with autoimmune disorders, inflammatory disease, acute myeloid leukemia, and solid tumors, it is expected as potential therapeutic target or biomarker. Relevance of the protein secretory pathway in the pathogenesis of known TRIB1-related diseases remains to be clarified in future investigations.

4 Conclusion and Outlook

Within a CRISPR based library screen, we discovered TRIB1 as novel orchestrator of the secretory pathway in myeloid cells. Our results indicate that within this pathway TRIB1 most likely controls Golgi well-function.

Following projects should aim to find out, which exact pathways within the Golgi apparatus are mediated by TRIB1. Golgi fragmentation and/or dispersal could be assessed via microscopy. Additionally, Golgi stress response of TRIB1 deficient cells should be investigated.

In the future our established system can be used to test possible protein trafficking defects in phenotypical patients with sequenced *TRIB1* mutations. Even though TRIB1 has been linked to multiple human diseases including various types of cancer (Liang, Rishi, & Keeshan, 2013; Wang et al., 2017; Yokoyama et al., 2012) and autoimmune diseases (Simoni et al., 2018) the exact molecular pathogenesis remains unsolved. As proper secretory trafficking plays a pivotal role in basic cell and tissue physiology, further studies regarding roles of TRIB1 in the secretory pathway could help elucidate a common ground for TRIB1 linked diseases and thus initiate novel approaches for therapeutic targets.

VII Summary

The secretory pathway plays a pivotal role for cell integrity and interaction. Even though our understanding towards organelle interaction and secretory trafficking has majorly improved, many questions remain unsolved. Especially considering the diversity of human pathologies, it remains crucial to further investigate basic cellular mechanisms and mediators of this pathway. Novel, progressive approaches combining bioinformatic approaches with large scale genome analyses help shed more light in this regard. Thus, CRISPR based large scale screens have initiated many novel findings in the genomic field. At the same time, matching the readout to clinical phenotypes has become a very powerful tool in translational research.

By applying a CRISPR library screen, we generated a large data set of genes, that are involved in protein secretory trafficking. We revised highly ranked genes from the screen and decided to specifically focus on *TRIB1* in this project. We constructed CD2 expressing *TRIB1* knockout cell lines by CRISPR/Cas9 targeting. Thereafter, we observed CD2 expression these cell lines by flow cytometry and visualized intracellular trafficking via immune fluorescence microscopy in *TRIB1* altered CD2 RUSH cell lines. In order to assess the recovery of the phenotype, we reconstituted *TRIB1* in all KO cell lines by lentiviral cloning. We furthermore investigated TRIB1's role in ER stress response using Tunicamycin.

In this project we discovered a novel function of TRIB1 within the secretory pathway, thereby confirming the result of our CRISPR library screen. We showed that protein trafficking was impaired by TRIB1 deletion and localized the trafficking error to the Golgi complex by imaging. Furthermore, we demonstrated, that this was a TRIB1 specific phenotype, since both CD2 cell surface expression and intracellular trafficking were restored by TRIB1 reconstitution. Additionally, we discovered, that TRIB1 does not play a role in UPR invoked by Tunicamycin.

In summary our work proposes TRIB1 as novel mediator of the secretory pathway, presumably on the Golgi level. More extensive research addressing the unique role of TRIB1 in Golgi homeostasis could help disclose a specific pathway of TRIB1 interaction.

In the clinical setting our established system could be used to assess trafficking defects in *TRIB1* mutated patients, linking TRIB1 related diseases to the secretory pathway. Due to TRIB1's role in basic cell biology, further research could help discover novel therapeutic targets in the future. In a larger context, this project demonstrates the relevance of large-scale screens in genomic research.

Zusammenfassung (Übersetzung in das Deutsche)

Die intakte Proteinsekretion spielt eine wesentliche Rolle für die Integrität und Interaktion von Zellen. Obwohl sich unser Verständnis für die Sekretionsmechanismen erheblich verbessert hat, bleiben weiterhin viele Fragen ungelöst. Da zahlreiche Erkrankungen mit einer gestörten Proteinsekretion einhergehen, ist die weitere Klärung dieser grundlegenden zellulären Mechanismen auch aus klinischer Sicht hoch relevant. Moderne Forschungsansätze, in denen bioinformatische Studien mit groß angelegten Genomanalysen kombiniert werden, können bei der Bearbeitung dieser Fragen hilfreich sein. So haben CRISPR-basierte Screenings bereits viele neue Erkenntnisse im Bereich der Genomik hervorgebracht. Gleichzeitig hat sich der Abgleich der Ergebnisse mit klinischen Phänotypen zu einem sehr leistungsfähigen Instrument für die translationale Forschung entwickelt.

Durch die Anwendung eines CRISPR-basierte Screenings wurde ein großer Datensatz von Genen generiert, die am sekretorischen Proteinverkehr beteiligt sind. Im Rahmen dieses Projektes erfolgte die manuelle Überprüfung des Genes *TRIB1*, welches einen hohen Rang in dem zuvor durchgeführten Screening erlangte. Hierfür wurden CD2-exprimierende *TRIB1*-Knockout-Zelllinien mittels der CRISPR/Cas9 Methode konstruiert. Anschließend wurde die CD2 Expression in diesen Zelllinien mittels Durchflusszytometrie untersucht. Zusätzlich wurde der intrazelluläre CD2 Transport mittels Immunfluoreszenzmikroskopie in CD2-RUSH-Zelllinien visualisiert. Um die Erholung des Phänotyps zu beurteilen, wurde *TRIB1* in allen Knockout-Zelllinien durch lenti-virale Klonierung wiederhergestellt. Darüber hinaus wurde die Rolle von *TRIB1* für die Stressreaktion des endoplasmatischen Retikulums erforscht.

Im Rahmen dieses Projektes konnte bestätigt werden, dass *TRIB1* eine Rolle für den intakten Proteintransport innerhalb der Zelle spielt. Wir konnten zeigen, dass der Proteintransport durch die Deletion von *TRIB1* beeinträchtigt ist und dass dies zu einer Proteinakkumulation im Golgiapparat führt. Darüber hinaus konnten wir nachweisen, dass es sich um einen *TRIB1*-spezifischen Phänotyp handelt, da sowohl die CD2 Expression auf der Zelloberfläche als auch der intrazelluläre Transport durch eine Rekonstitution von *TRIB1* wiederhergestellt werden konnten.

Zusammenfassend wurde in dieser Arbeit eine neue Funktion des Genes *TRIB1* – als Vermittler im Proteintransport – entdeckt. Anknüpfende Projekte könnten dazu beitragen einen spezifischen Weg der *TRIB1* Interaktion zu untersuchen. Im klinischen Umfeld könnte unser etabliertes System zur Überprüfung von Transportdefekten bei Patienten mit *TRIB1* Mutationen eingesetzt werden, um einen möglichen Zusammenhang zwischen *TRIB1* assoziierten Erkrankungen und gestörtem Proteintransport zu beleuchten. Langfristig könnte dies dazu beitragen neue Therapieansätze zu generieren. Im größeren Kontext demonstriert diese Arbeit die Relevanz von groß angelegten Screenings für die Genomforschung.

VIII Table Index

Tab. 1 Kits 15

Tab. 2 Substances 15

Tab. 3 Buffers 17

Tab. 4 CRISPR/Cas9 guide sequences 19

Tab. 5 Primers for seqencing 19

Tab. 6 Primers for cloning 19

Tab. 7 Primers for genome check 19

Tab. 8 Primers for RT-PCR 20

Tab. 9 Plasmids 20

Tab. 10 Cell lines and bacteria strains 20

Tab. 11 Components of running and stacking gel for SDS-PAGE 31

IX Figure Index

Fig. 1 CRISPR/Cas9 methodology scheme. 12

Fig. 2 LentiCRISPRv2 vector. 21

Fig. 3 pMiniT2.0 cloning vector. 22

Fig. 4 HA-IRES-RFP-pRRL lentiviral vector. 23

Fig. 5 RUSH system in GFP tagged CD2 KBM7 RUSH cells. 28

Fig. 6 CD2-RUSH-pRRL vector for KBM7 cell transduction.. 29

Fig. 7 *TRIB1* gene. 33

Fig. 8 Constructed lentiCRISPRv2 vector for *TRIB1* targeting. 34

Fig. 9 Exemplary PCR of *TRIB1* target locus in different single cell clones using Onetaq. 34

Fig. 10 Chromatogram of *TRIB1* target locus in lentiCRISPRv2-TRIB1 transduced cells. 35

Fig. 11 FACS analysis of CD2 expressing KBM7 cells targeted with gRNA1.. 36

Fig. 12 FACS analysis of CD2 expressing KBM7 cells targeted with gRNA2.. 37

Fig. 13 MluI-TRIB1-SfaAI amplicon.. 38

Fig. 14 Constructed MluI-TRIB1-SfaAI-pMiniT2.0 cloning vector for *TRIB1* reconstitution 38

Fig. 15 Digestion of MluI-TRIB1-SfaAI-pMiniT2.0 cloning vector using MluI and SfaAI. 39

Fig. 16 TRIB1-HA-IRES-RFP-pRRL vector cloning for *TRIB1* reconstitution. 39

Fig. 17 RT-PCR of TRIB1 cDNA in CD2 KBM7 cell clones. 40

Fig. 18 FACS analysis of CD2 expressing KBM7 cells upon *TRIB1* reconstitution 42

Fig. 19 Confocal imaging of CD2-RUSH-KBM7 cells. 46

Fig. 20 RT-PCR of UPR genes after Tunicamycin treatment. 47

X References

Acharya, U., Mallabiabarrena, A., Acharya, J. K., & Malhotra, V. (1998). Signaling via mitogen-activated protein kinase kinase (MEK1) is required for Golgi fragmentation during mitosis. *Cell*, *92*(2), 183–192. https://doi.org/10.1016/S0092-8674(00)80913-7

Amara, J. F., Cheng, S. H., & Smith, A. E. (1992). Intracellular protein trafficking defects in human disease. *Trends in Cell Biology*, *2*(5), 145–149. https://doi.org/10.1016/0962-8924(92)90101-R

Aridor, M., & Hannan, L. A. (2002). Traffic Jams II: An update of diseases of intracellular transport. *Traffic*, *3*(11), 781–790. https://doi.org/10.1034/j.1600-0854.2002.31103.x

Arndt, L., Dokas, J., Gericke, M., Kutzner, C. E., Müller, S., Jeromin, F., Thiery, J., & Burkhardt, R. (2018). Tribbles homolog 1 deficiency modulates function and polarization of murine bone marrow– derived macrophages. *Journal of Biological Chemistry*, *293*(29), 11527–11536. https://doi.org/10.1074/jbc.RA117.000703

Baker, K. E., & Parker, R. (2004). Nonsense-mediated mRNA decay: Terminating erroneous gene expression. *Current Opinion in Cell Biology*, *16*(3), 293–299. https://doi.org/10.1016/j.ceb.2004.03.003

Barinaga-Rementeria Ramirez, I., & Lowe, M. (2009). Golgins and GRASPs: Holding the Golgi together. *Seminars in Cell and Developmental Biology*, *20*(7), 770–779. https://doi.org/10.1016/j.semcdb.2009.03.011

Barrangou, R., & Doudna, J. A. (2016). Applications of CRISPR technologies in research and beyond. *Nature Biotechnology*, *34*(9), 933–941. https://doi.org/10.1038/nbt.3659

Baschieri, F., Confalonieri, S., Bertalot, G., Di Fiore, P. P., Dietmaier, W., Leist, M., Crespo, P., Macara, I. G., & Farhan, H. (2015). Spatial control of Cdc42 signalling by a GM130-RasGRF complex regulates polarity and tumorigenesis. *Nature Communications*, *5*, 139–148. https://doi.org/doi:10.1038/ncomms5839

Bednarek, S. Y., & Raikhel, N. V. (1992). Intracellular trafficking of secretory proteins. *Plant Molecular Biology*, *20*(1), 133–150. https://doi.org/10.1007/BF00029156

Bisel, B., Wang, Y., Wei, J. H., Xiang, Y., Tang, D., Miron-Mendoza, M., Yoshimura, S. I., Nakamura, N., & Seemann, J. (2008). ERK regulates Golgi and centrosome orientation towards the leading edge through GRASP65. *Journal of Cell Biology*, *182*(5), 837–843. https://doi.org/10.1083/jcb.200805045

Boncompain, G., Divoux, S., Gareil, N., De Forges, H., Lescure, A., Latreche, L., Mercanti, V., Jollivet, F., Raposo, G., & Perez, F. (2012). Synchronization of secretory protein traffic in populations of cells. *Nature Methods*, *9*(5), 493–498. https://doi.org/10.1038/nmeth.1928

Boncompain, G., & Perez, F. (2013). The many routes of Golgi-dependent trafficking. *Histochemistry and Cell Biology*, *140*(3), 251–260. https://doi.org/10.1007/s00418-013-1124-7

Boncompain, G., & Weigel, A. V. (2018). Transport and sorting in the Golgi complex: multiple mechanisms sort diverse cargo. *Current Opinion in Cell Biology*, *50*, 94–101. https://doi.org/10.1016/j.ceb.2018.03.002

Bryant, D. M., & Yap, A. S. (2016). Editorial overview: Membrane traffic and cell polarity. *Traffic*, *17*(12), 1231–1232. https://doi.org/10.1111/tra.12433

Bukau, B., Weissman, J., & Horwich, A. (2006). Molecular Chaperones and Protein Quality Control. *Cell*, *125*(3), 443–451. https://doi.org/10.1016/j.cell.2006.04.014

Calfon, M., Zeng, H., Urano, F., Till, J. H., Hubbard, S. R., Harding, H. P., Clark, S. G., & Ron, D. (2002). IRE1 couples endoplasmic reticulum load to secretory capacity by processing the XBP-1 mRNA. *Nature*, *415*(6867), 92–96. https://doi.org/10.1038/415092a

Carter, M., & Shieh, J. (2015). Molecular Cloning and Recombinant DNA Technology. *Guide to Research Techniques in Neuroscience*, *1*, 219–237. https://doi.org/10.1016/b978-0-12-800511-8.00010-1

Chen, H., Li, M., Sanchez, E., Soof, C. M., Bujarski, S., Ng, N., Cao, J., Hekmati, T., Zahab, B., Nosrati, J. D., Wen, M., Wang, C. S., Tang, G., Xu, N., Spektor, T. M., & Berenson, J. R. (2020). JAK1/2 pathway inhibition suppresses M2 polarization and overcomes resistance of myeloma to lenalidomide by reducing TRIB1, MUC1, CD44, CXCL12, and CXCR4 expression. *British Journal of Haematology*, *188*(2), 283–294. https://doi.org/10.1111/bjh.16158

Danger, R., Feseha, Y., & Brouard, S. (2022). The Pseudokinase TRIB1 in Immune Cells and Associated Disorders. *Cancers*, *14*(5), 196–224. https://doi.org/https://doi.org/10.3390/cancers14041011

Dedhia, P. H., Keeshan, K., Uljon, S., Xu, L., Vega, M. E., Shestova, O., Zaks-Zilberman, M., Romany, C., Blacklow, S. C., & Pear, W. S. (2010). Differential ability of Tribbles family members to promote degradation of C/EBPα and induce acute myelogenous leukemia. *Blood*, *116*(8), 1321–1328. https://doi.org/10.1182/blood-2009-07-229450

Dobson, C. M. (2003). Protein folding and misfolding. *Nature*, *426*(6968), 884–890. https://doi.org/10.1038/nature02261

Doudna, J. A., & Charpentier, E. (2014). The new frontier of genome engineering with CRISPR-Cas9. *Science*, *346*(6213). https://doi.org/10.1126/science.1258096

Duan, J., Lu, G., Xie, Z., Lou, M., Luo, J., Guo, L., & Zhang, Y. (2014). Genome-wide identification of CRISPR/Cas9 off-targets in human genome. *Cell Research*, *24*(8), 1009–1012. https://doi.org/10.1038/cr.2014.87

Ellgaard, L., & Helenius, A. (2003). Quality control in the endoplasmic reticulum. *Nature Reviews Molecular Cell Biology*, *4*(3), 181–191. https://doi.org/10.1038/nrm1052

Eyers, P. A. (2015). TRIBBLES: A Twist in the Pseudokinase Tail. *Structure*, *23*(11), 1974–1976. https://doi.org/10.1016/j.str.2015.10.003

Eyers, P. A., Keeshan, K., & Kannan, N. (2017). Tribbles in the 21st Century: The Evolving Roles of Tribbles Pseudokinases in Biology and Disease. *Trends in Cell Biology*, *27*(4), 284–298. https://doi.org/10.1016/j.tcb.2016.11.002

Fellmann, C., Gowen, B. G., Lin, P. C., Doudna, J. A., & Corn, J. E. (2017). Cornerstones of CRISPR-Cas in drug discovery and therapy. *Nature Reviews Drug Discovery*, *16*(2), 89–100. https://doi.org/10.1038/nrd.2016.238

Fu, Y., Foden, J. A., Khayter, C., Maeder, M. L., Reyon, D., Joung, K. J., & Sander, J. D. (2013). High-frequency off-target mutagenesis induced by CRISPR-Cas nucleases in human cells. *Nature Biotechnology*, *31*(9), 851–857. https://doi.org/10.1038/nbt.2623

Garneau, N. L., Wilusz, J., & Wilusz, C. J. (2007). The highways and byways of mRNA decay. *Nature Reviews Molecular Cell Biology*, *8*(2), 113–126. https://doi.org/10.1038/nrm2104

Gregersen, N., Bross, P., Vang, S., & Christensen, J. H. (2006). Protein Misfolding and Human Disease. *Annual Review of Genomics and Human Genetics*, *7*(1), 103–124. https://doi.org/10.1146/annurev.genom.7.080505.115737

Guo, Y., Sirkis, D. W., & Schekman, R. (2014). Protein Sorting at the trans -Golgi Network . *Annual Review of Cell and Developmental Biology*, *30*(1), 169–206. https://doi.org/10.1146/annurev-cellbio-100913-013012

Han, J., Back, S. H., Hur, J., Lin, Y. H., Gildersleeve, R., Shan, J., Yuan, C. L., Krokowski, D., Wang, S., Hatzoglou, M., Kilberg, M. S., Sartor, M. A., & Kaufman, R. J. (2013). ER-stress-induced transcriptional regulation increases protein synthesis leading to cell death. *Nature Cell Biology*, *15*(5), 481–490. https://doi.org/10.1038/ncb2738

Han, J., & Kaufman, R. J. (2014). Measurement of the unfolded protein response to investigate its role in adipogenesis and obesity. In *Methods in Enzymology* (1st ed., Vol. 538). Elsevier Inc. https://doi.org/10.1016/B978-0-12-800280-3.00008-6

Harding, H. P., Zhang, Y., Zeng, H., Novoa, I., Lu, P. D., Calfon, M., Sadri, N., Yun, C., Popko, B., Paules, R., Stojdl, D. F., Bell, J. C., Hettmann, T., Leiden, J. M., & Ron, D. (2003). An integrated stress response regulates amino acid metabolism and resistance to oxidative stress. *Molecular Cell*, *11*(3), 619–633. https://doi.org/10.1016/S1097-2765(03)00105-9

Haze, K., Yoshida, H., Yanagi, H., Yura, T., & Mori, K. (1999). Mammalian transcription factor ATF6 is synthesized as a transmembrane protein and activated by proteolysis in response to endoplasmic reticulum stress. *Molecular Biology of the Cell*, *10*(11), 3787–3799. https://doi.org/10.1091/mbc.10.11.3787

Hernández-Quiles, M., Baak, R., Borgman, A., Den Haan, S., Alcaraz, P. S., Van Es, R., Kiss-Toth, E., Vos, H., & Kalkhoven, E. (2021). Comprehensive profiling of mammalian tribbles interactomes implicates TRIB3 in gene repression. *Cancers*, *13*(24). https://doi.org/10.3390/cancers13246318

Hetz, C., & Mollereau, B. (2014). Disturbance of endoplasmic reticulum proteostasis in neurodegenerative diseases. *Nature Reviews Neuroscience*, *15*(4), 233–249. https://doi.org/10.1038/nrn3689

Hsu, P. D., Scott, D. A., Weinstein, J. A., Ran, F. A., Konermann, S., Agarwala, V., Li, Y., Fine, E. J., Wu, X., Shalem, O., Cradick, T. J., Marraffini, L. A., Bao, G., & Zhang, F. (2013). DNA targeting specificity of RNA-guided Cas9 nucleases. *Nature Biotechnology*, *31*(9), 827–832. https://doi.org/10.1038/nbt.2647

Jamieson, S. A., Ruan, Z., Burgess, A. A., Curry, J. R., McMillan, H. D., Brewster, J. L., Dunbier, A. K., Axtman, A. D., Kannan, N., & Mace, P. D. (2019). Substrate binding allosterically relieves autoinhibition of the pseudikinase TRIB1. *Science Signaling*, *11*(1549). https://doi.org/10.1126/scisignal.aau0597

Jansen, J. C., Cirak, S., Van Scherpenzeel, M., Timal, S., Reunert, J., Rust, S., Pérez, B., Vicogne, D., Krawitz, P., Wada, Y., Ashikov, A., Pérez-Cerdá, C., Medrano, C., Arnoldy, A., Hoischen, A., Huijben, K., Steenbergen, G., Quelhas, D., Diogo, L., … Lefeber, D. J. (2016). CCDC115 Deficiency Causes a Disorder of Golgi Homeostasis with Abnormal Protein Glycosylation. *American Journal of Human Genetics*, *98*(2), 310–321. https://doi.org/10.1016/j.ajhg.2015.12.010

Jin, G., Yamazaki, Y., Takuwa, M., Takahara, T., Kaneko, K., Kuwata, T., Miyata, S., & Nakamura, T. (2007). Trib1 and Evi1 cooperate with Hoxa and Meis1 in myeloid leukemogenesis. *Blood*, *109*(9), 3998–4005. https://doi.org/10.1182/blood-2006-08-041202

Jostins, L., Ripke, S., Weersma, R. K., Duerr, R. H., McGovern, D. P., Hui, K. Y., Lee, J. C., Philip Schumm, L., Sharma, Y., Anderson, C. A., Essers, J., Mitrovic, M., Ning, K., Cleynen, I., Theatre, E., Spain, S. L., Raychaudhuri, S., Goyette, P., Wei, Z., … Whittaker, P. (2012). Host-microbe interactions have shaped the genetic architecture of inflammatory bowel disease. *Nature*, *491*(7422), 119–124. https://doi.org/10.1038/nature11582

Kiessling, M. K., Schuierer, S., Stertz, S., Beibel, M., Bergling, S., Knehr, J., Carbone, W., de Vallière, C., Tchinda, J., Bouwmeester, T., Seuwen, K., Rogler, G., & Roma, G. (2016). Identification of oncogenic driver mutations by genome-wide CRISPR-Cas9 dropout screening. *BMC Genomics*, *17*(1), 1–16. https://doi.org/10.1186/s12864-016-3042-2

Kiss-Toth, E., Bagstaff, S. M., Sung, H. Y., Jozsa, V., Dempsey, C., Caunt, J. C., Oxley, K. M., Wyllie, D. H., Polgar, T., Harte, M., O'Neil, L. A. J., Qwarnstrom, E. E., & Dower, S. E. (2004). Human tribbles, a protein family controlling mitogen-activated protein kinase cascades. *Journal of Biological Chemistry*, *279*(41), 42703–42708. https://doi.org/10.1074/jbc.M407732200

Klumperman, J. (2011). Architecture of the mammalian Golgi. *Cold Spring Harbor Perspectives in Biology*, *3*(7), 1–19. https://doi.org/10.1101/cshperspect.a005181

Koike-Yusa, H., Li, Y., Tan, E. P., Velasco-Herrera, M. D. C., & Yusa, K. (2014). Genome-wide recessive genetic screening in mammalian cells with a lentiviral CRISPR-guide RNA library. *Nature Biotechnology*, *32*(3), 267–273. https://doi.org/10.1038/nbt.2800

Korkmaz, G., Lopes, R., Ugalde, A. P., Nevedomskaya, E., Han, R., Myacheva, K., Zwart, W., Elkon, R., & Agami, R. (2016). Functional genetic screens for enhancer elements in the human genome using CRISPR-Cas9. *Nature Biotechnology*, *34*(2), 192–198. https://doi.org/10.1038/nbt.3450

Kung, J. E., & Jura, N. (2019). The pseudokinase TRIB 1 toggles an intramolecular switch to regulate COP 1 nuclear export . *The EMBO Journal*, *38*(4), 1–16. https://doi.org/10.15252/embj.201899708

Kuscu, C., Arslan, S., Singh, R., Thorpe, J., & Adli, M. (2014). Genome-wide analysis reveals characteristics of off-target sites bound by the Cas9 endonuclease. *Nature Biotechnology*, *32*(7), 677–683. https://doi.org/10.1038/nbt.2916

Liang, K. L., Rishi, L., & Keeshan, K. (2013). Blood Spotlight Tribbles in acute leukemia. *Blood*, *121*(21), 4265–4270. https://doi.org/10.1182/blood-2012-12-471300.The

Machamer, C. E. (2015). The Golgi complex in stress and death. *Frontiers in Neuroscience*, *9*(NOV), 1–5. https://doi.org/10.3389/fnins.2015.00421

Mack, E. A., Stein, S. J., Rome, K. S., Xu, L., Wertheim, G. B., Melo, R. C. N., & Pear, W. S. (2019). Trib1 regulates eosinophil lineage commitment and identity by restraining the neutrophil program. *Blood*, *133*(22), 2413–2426. https://doi.org/10.1182/blood.2018872218

Makhoul, C., Gosavi, P., & Gleeson, P. A. (2019). Golgi Dynamics: The Morphology of the Mammalian Golgi Apparatus in Health and Disease. *Frontiers in Cell and Developmental Biology*, *7*(July), 1–7. https://doi.org/10.3389/fcell.2019.00112

Marciniak, S. J., Yun, C. Y., Oyadomari, S., Novoa, I., Zhang, Y., Jungreis, R., Nagata, K., Harding, H. P., & Ron, D. (2004). CHOP induces death by promoting protein synthesis and oxidation in the stressed endoplasmic reticulum. *Genes and Development*, *18*(24), 3066–3077. https://doi.org/10.1101/gad.1250704

Marra, P., Salvatore, L., Mironov, A., Di Campli, A., De Matteis, M. A., Chieti, & Italy. (2007). The Biogenesis of the Golgi Ribbon: The Roles of Membrane Input from the ER and of GM130. *Molecular Biology of the Cell*, *18*(March), 976–985. https://doi.org/10.1091/mbc.E06

Mashima, T., Soma-Nagae, T., Migita, T., Kinoshita, R., Iwamoto, A., Yuasa, T., Yonese, J., Ishikawa, Y., & Seimiya, H. (2014). TRIB1 supports prostate tumorigenesis and tumor-propagating cell survival by regulation of endoplasmic reticulum chaperone expression. *Cancer Research*, *74*(17), 4888–4897. https://doi.org/10.1158/0008-5472.CAN-13-3718

McMillan, H. D., Keeshan, K., Dunbier, A. K., & Mace, P. D. (2021). Structure vs. Function of trib1—myeloid neoplasms and beyond. *Cancers*, *13*(12). https://doi.org/10.3390/cancers13123060

Murphy, J. M., Nakatani, Y., Jamieson, S. A., Dai, W., Lucet, I. S., & Mace, P. D. (2015). Molecular Mechanism of CCAAT-Enhancer Binding Protein Recruitment by the TRIB1 Pseudokinase. *Structure*, *23*(11), 2111–2121. https://doi.org/10.1016/j.str.2015.08.017

Nickel, W., & Rabouille, C. (2009). Mechanisms of regulated unconventional protein secretion. *Nature Reviews Molecular Cell Biology*, *10*(2), 148–155. https://doi.org/10.1038/nrm2617

Park, H., Shin, D. H., Sim, J. R., Aum, S., & Lee, M. G. (2020). IRE1α kinase–mediated unconventional protein secretion rescues misfolded CFTR and pendrin. *Science Advances*, *6*(8). https://doi.org/10.1126/sciadv.aax9914

Parnas, O., Jovanovic, M., Eisenhaure, T. M., Herbst, R. H., Dixit, A., Ye, C. J., Przybylski, D., Platt, R. J., & Tirosh, I. (2015). A genome-wide CRISPR screen in primary immune cells to dissect regulatory networks. *Cell*, *162*(3), 675–686. https://doi.org/10.1016/j.cell.2015.06.059.A

Pattanayak, V., Lin, S., Guilinger, J. P., Ma, E., Doudna, J. A., & Liu, D. R. (2013). High-throughput profiling of off-target DNA cleavage reveals RNA-programmed Cas9 nuclease specificity. *Nature Biotechnology*, *31*(9). https://doi.org/10.1016/j.physbeh.2017.03.040

Rabouille, C., & Kondylis, V. (2007). Golgi ribbon unlinking: An organelle-based G2/M checkpoint. *Cell Cycle*, *6*(22), 2723–2729. https://doi.org/10.4161/cc.6.22.4896

Ran, F. A., Hsu, P. D., Wright, J., Agarwala, V., Scott, D. A., & Zhang, F. (2013). Genome engineering using the CRISPR-Cas9 system. *Nature Protocols*, *8*(11), 2281–2308. https://doi.org/10.1038/nprot.2013.143

Ravichandran, Y., Goud, B., & Manneville, J. B. (2020). The Golgi apparatus and cell polarity: Roles of the cytoskeleton, the Golgi matrix, and Golgi membranes. *Current Opinion in Cell Biology*, *62*, 104–113. https://doi.org/10.1016/j.ceb.2019.10.003

Reiling, J. H., Clish, C. B., Carette, J. E., Varadarajan, M., Brummelkamp, T. R., & Sabatini, D. M. (2011). A haploid genetic screen identifies the major facilitator domain containing 2A (MFSD2A) transporter as a key mediator in the response to tunicamycin. *Proceedings of the National Academy of Sciences of the United States of America*, *108*(29), 11756–11765. https://doi.org/10.1073/pnas.1018098108

Röthlisberger, B., Heizmann, M., Bargetzi, M. J., & Huber, A. R. (2007). TRIB1 overexpression in acute myeloid leukemia. *Cancer Genetics and Cytogenetics*, *176*(1), 58–60. https://doi.org/10.1016/j.cancergencyto.2007.03.003

Rothman, J. E., & Orci, L. (1992). Molecular dissection of the secretory pathway. *Nature*, *355*(6359), 409–415. https://doi.org/10.1038/355409a0

Satoh, T., Kidoya, H., Naito, H., Yamamoto, M., Takemura, N., Nakagawa, K., Yoshioka, Y., Morii, E., Takakura, N., Takeuchi, O., & Akira, S. (2013). Critical role of Trib1 in differentiation of tissue-resident M2-like macrophages. *Nature*, *495*(7442), 524–528. https://doi.org/10.1038/nature11930

Shahrouzi, P., Astobiza, I., Cortazar, A. R., Torrano, V., Macchia, A., Flores, J. M., Niespolo, C., Mendizabal, I., Caloto, R., Ercilla, A., Camacho, L., Arreal, L., Bizkarguenaga, M., Martinez-Chantar, M. L., Bustelo, X. R., Berra, E., Kiss-Toth, E., Velasco, G., Zabala-Letona, A., & Carracedo, A. (2020). Genomic and Functional Regulation of TRIB1 Contributes to Prostate Cancer Pathogenesis. *Cancers*, *12*(9), 2593. https://doi.org/10.3390/cancers12092593

Silva, R. M., Ries, V., Oo, T. F., Yarygina, O., Jackson-Lewis, V., Ryu, E. J., Lu, P. D., Marciniak, S. J., Ron, D., Przedborski, S., Kholodilov, N., Greene, L. A., & Burke, R. E. (2005). CHOP/GADD153 is a mediator of apoptotic death in substantia nigra dopamine neurons in an in vivo neurotoxin model of parkinsonism. *Journal of Neurochemistry*, *95*(4), 974–986. https://doi.org/10.1111/j.1471-4159.2005.03428.x

Simoni, L., Delgado, V., Ruer-Laventie, J., Bouis, D., Soley, A., Heyer, V., Robert, I., Gies, V., Martin, T., Korganow, A. S., San Martin, B. R., & Soulas-Sprauel, P. (2018). Trib1 is overexpressed in systemic lupus erythematosus, while it regulates immunoglobulin production in murine B cells. *Frontiers in Immunology*, *9*(MAR). https://doi.org/10.3389/fimmu.2018.00373

Sitia, R., & Braakman, I. (2003). Quality control in the endoplasmic reticulum protein factory. *Nature*, *426*(6968), 891–894. https://doi.org/10.1038/nature02262

Smith, M. H., Ploegh, H. L., & Weissman, J. S. (2011). Road to ruin: Targeting proteins for degradation in the endoplasmic reticulum. *Science*, *334*(6059), 1086–1090. https://doi.org/10.1126/science.1209235

Soubeyrand, S., Martinuk, A., Lau, P., & McPherson, R. (2016). TRIB1 is regulated post-transcriptionally by proteasomal and non-proteasomal pathways. *PLoS ONE*, *11*(3), 1–21. https://doi.org/10.1371/journal.pone.0152346

Sütterlin, C., Hsu, P., Mallabiabarrena, A., & Malhotra, V. (2002). Fragmentation and dispersal of the pericentriolar Golgi complex is required for entry into mitosis in mammalian cells. *Cell*, *109*(3), 359–369. https://doi.org/10.1016/S0092-8674(02)00720-1

Toledo, C. M., Ding, Y., Hoellerbauer, P., Davis, R. J., Basom, R., Girard, E. J., Lee, E., Corrin, P., Hart, T., Bolouri, H., Davison, J., Zhang, Q., Hardcastle, J., Aronow, B. J., Plaisier, C. L., Baliga, N. S., Moffat, J., Lin, Q., Li, X. N., … Paddison, P. J. (2015). Genome-wide CRISPR-Cas9 Screens Reveal Loss of Redundancy between PKMYT1 and WEE1 in Glioblastoma Stem-like Cells. *Cell Reports*, *13*(11), 2425–2439. https://doi.org/10.1016/j.celrep.2015.11.021

Tuladhar, R., Yeu, Y., Tyler Piazza, J., Tan, Z., Rene Clemenceau, J., Wu, X., Barrett, Q., Herbert, J., Mathews, D. H., Kim, J., Hyun Hwang, T., & Lum, L. (2019). CRISPR-Cas9-based mutagenesis frequently provokes on-target mRNA misregulation. *Nature Communications*, *10*(1), 1–10. https://doi.org/10.1038/s41467-019-12028-5

Uchiyama, K., Muramatsu, N., Yano, M., Usui, T., Miyata, H., & Sakaguchi, S. (2013). Prions disturb post-Golgi trafficking of membrane proteins. *Nature Communications*, *4*(May). https://doi.org/10.1038/ncomms2873

Van Bergen, N. J., Guo, Y., Al-Deri, N., Lipatova, Z., Stanga, D., Zhao, S., Murtazina, R., Gyurkovska, V., Pehlivan, D., Mitani, T., Gezdirici, A., Antony, J., Collins, F., Willis, M. J. H., Akdemir, Z. H. C., Liu, P., Punetha, J., Hunter, J. V., Jhangiani, S. N., … Christodoulou, J. (2020). Deficiencies in vesicular transport mediated by TRAPPC4 are associated with severe syndromic intellectual disability. *Brain*, *143*(1), 112–130. https://doi.org/10.1093/brain/awz374

Walter, P., & Ron, D. (2011). The unfolded protein response: From stress pathway to homeostatic regulation. *Science*, *334*(6059), 1081–1086. https://doi.org/10.1126/science.1209038

Wang, M., & Kaufman, R. J. (2014). The impact of the endoplasmic reticulum protein-folding environment on cancer development. *Nature Reviews Cancer*, *14*(9), 581–597. https://doi.org/10.1038/nrc3800

Wang, S., & Kaufman, R. J. (2012). The impact of the unfolded protein response on human disease. *Journal of Cell Biology*, *197*(7), 857–867. https://doi.org/10.1083/jcb.201110131

Wang, T., Wei, J. J., Sabatini, D. M., & Lander, E. S. (2012). Genetic screens in human cells using the CRISPR-Cas9 system. *BMJ Supportive and Palliative Care*, *2*(3), 256–263. https://doi.org/10.1136/bmjspcare-2011-000063

Wang, Y., Wu, N., Pang, B., Tong, D., Sun, D., Sun, H., Zhang, C., Sun, W., Meng, X., Bai, J., Chen, F., Geng, J., Fu, S., & Jin, Y. (2017). TRIB1 promotes colorectal cancer cell migration and invasion through activation MMP-2 via FAK/Src and ERK pathways. *Oncotarget*, *8*(29), 47931–47942. https://doi.org/10.18632/oncotarget.18201

Wu, J., Rutkowski, D. T., Dubois, M., Swathirajan, J., Saunders, T., Wang, J., Song, B., Yau, G. D. Y., & Kaufman, R. J. (2007). ATF6α Optimizes Long-Term Endoplasmic Reticulum Function to Protect Cells from Chronic Stress. *Developmental Cell*, *13*(3), 351–364. https://doi.org/10.1016/j.devcel.2007.07.005

Ye, Y., Wang, G., Wang, G., Zhuang, J., He, S., Song, Y., Ni, J., Xia, W., & Wang, J. (2017). The oncogenic role of Tribbles 1 in hepatocellular carcinoma is mediated by a feedback loop involving microRNA-23a and p53. *Frontiers in Physiology*, *8*(NOV), 1–11. https://doi.org/10.3389/fphys.2017.00789

Yokoyama, T., Kanno, Y., Yamazaki, Y., Takahara, T., Miyata, S., & Nakamura, T. (2010). Trib1 links the MEK1/ERK pathway in myeloid leukemogenesis. *Blood*, *116*(15), 2768–2775. https://doi.org/10.1182/blood-2009-10-246264

Yokoyama, T., Toki, T., Aoki, Y., Kanezaki, R., Park, M. J., Kanno, Y., Takahara, T., Yamazaki, Y., Ito, E., Hayashi, Y., & Nakamura, T. (2012). Identification of TRIB1 R107L gain-of-function mutation in human acute megakaryocytic leukemia. *Blood*, *119*(11), 2608–2611. https://doi.org/10.1182/blood-2010-12-324806

Yoshida. (2013). COP1 targets C / EBP a for degradation and induces acute myeloid myeloid leukemia via Trib1. *Blood*, *122*(10), 1750–1760. https://doi.org/10.1182/blood-2012-12-476101.component

Yoshino, S., Yokoyama, T., Sunami, Y., Takahara, T., Nakamura, A., Yamazaki, Y., Tsutsumi, S., Aburatani, H., & Nakamura, T. (2021). Trib1 promotes acute myeloid leukemia progression by modulating the transcriptional programs of Hoxa9. *Blood*, *137*(1), 75–88. https://doi.org/10.1182/blood.2019004586

Zhang, K., & Kaufman, R. J. (2008). From endoplasmic-reticulum stress to the inflammatory response. *Nature*, *454*(7203), 455–462. https://doi.org/10.1038/nature07203

Zhang, X. H., Tee, L. Y., Wang, X. G., Huang, Q. S., & Yang, S. H. (2015). Off-target effects in CRISPR/Cas9-mediated genome engineering. *Molecular Therapy - Nucleic Acids*, *4*(11), e264. https://doi.org/10.1038/mtna.2015.37

XI Appendix

1 Acknowledgements

My heartfelt thanks go to Prof. Dr. Christoph Klein for the opportunity to carry out my medical doctorate thesis under his excellent supervision as well as his constant support and encouragement.

I would like to especially thank Dr. Megumi Tatematsu for her outstanding supervision of my work, her continuous guidance during these last years, her constant enthusiasm and her moral support far beyond that. Thank you for the great cooperation. This thesis would not have been possible without you.

Furthermore, I would like to thank all members of the Klein Lab for their help and support in the laboratory, for the pleasant working atmosphere and the social activities outside of work. Special thanks go to my colleagues Dr. med. Stella Bergemann, Dr. Yoko Mizoguchi, Yanxin Fan, Laura Frey, David Illig, Dr. Felipe Romero and Dr. Diana Romero for many encouraging conversations, valuable ideas and their constant willingness to help.

Finally, I would like to thank my family and friends for always having an open ear and for always being by my side. Your encouraging words, emotional support and constant presence carried me through this thesis. Above all, I would like to thank my parents for their great support and guidance in every situation.

2 Affidavit

LMU

LUDWIG-
MAXIMILIANS-
UNIVERSITÄT
MÜNCHEN

Promotionsbüro
Medizinische Fakultät

MMRS

Eidesstattliche Versicherung

Gan, Anna Lu

Name, Vorname

Ich erkläre hiermit an Eides statt, dass ich die vorliegende Dissertation mit dem Titel:

Identification of TRIB1 as a Novel Regulator of the Secretory Pathway

selbständig verfasst, mich außer der angegebenen keiner weiteren Hilfsmittel bedient und alle Erkenntnisse, die aus dem Schrifttum ganz oder annähernd übernommen sind, als solche kenntlich gemacht und nach ihrer Herkunft unter Bezeichnung der Fundstelle einzeln nachgewiesen habe.

Ich erkläre des Weiteren, dass die hier vorgelegte Dissertation nicht in gleicher oder in ähnlicher Form bei einer anderen Stelle zur Erlangung eines akademischen Grades eingereicht wurde.

München, 01.07.2023 Anna Lu Gan

Ort, Datum Unterschrift Doktorandin bzw. Doktorand